



Experimental assessment of the sensitivity of an estuarine phytoplankton fall bloom to acidification and warming

Robin Bénard¹, Maurice Levasseur¹, Michael Grant Scarratt², Marie-Amélie Blais¹, Alfonso Mucci³, Gustavo Ferreyra⁴, Michel Starr², Michel Gosselin⁴, Jean-Éric Tremblay¹, Martine Lizotte¹

¹Département de biologie, Université Laval, 1045 avenue de la Médecine, Québec, Québec G1V 0A6, Canada

²Fisheries and Oceans Canada, Maurice Lamontagne Institute, P.O. Box 1000, Mont-Joli, Québec G5H 3Z4, Canada

³Department of Earth and Planetary Sciences, McGill University, 3450 University Street, Montréal, Québec H3A 2A7, Canada

⁴Institut des sciences de la mer de Rimouski (ISMER), Université du Québec à Rimouski, 310 allée des Ursulines, Rimouski, Québec G5L 3A1, Canada

Correspondence: Robin Bénard (robin.benard.1@ulaval.ca)

Abstract. We investigated the combined effect of ocean acidification and warming on the dynamics of the phytoplankton fall bloom in the Lower St. Lawrence Estuary (LSLE), Canada. Twelve 2600 L mesocosms were set to initially cover a wide range of pH_T (pH on the total proton scale) from 8.0 to 7.2 corresponding to a range of pCO₂ from 440 to 2900 µatm, and two temperatures (in situ and +5 °C). The 13-day experiment captured the development and decline of a nanophytoplankton bloom dominated by the chain-forming diatom *Skeletonema costatum*. During the development phase of the bloom, increasing pCO₂ influenced neither the magnitude nor the net growth rate of the nanophytoplankton bloom whereas increasing the temperature by 5 °C stimulated the chlorophyll *a* (Chl *a*) growth rate and particulate primary production (P_p) by 50 % and 160 %, respectively. During the declining phase of the bloom, warming accelerated the loss of diatom cells and negatively affected P_p. Due to the countervailing responses of the plankton community to warming during the two phases of the experiment, the time-integrated primary production was not significantly affected over the full duration of the study. The diatom bloom was paralleled by a gradual decrease in the abundance of photosynthetic picoeukaryotes and followed by a bloom of picocyanobacteria. Increasing pCO₂ and warming did not influence the abundance of picoeukaryotes, but warming stimulated picocyanobacteria proliferation. Overall, our results suggest that warming, rather than acidification, is more likely to alter phytoplankton autumnal bloom development in the LSLE in the decades to come. Future studies examining a broader gradient of temperatures should be conducted over a larger seasonal window in order to better constrain the potential effect of warming on the development of blooms in the LSLE and its impact on the fate of primary production.

1. Introduction

Anthropogenic emissions have increased atmospheric carbon dioxide (CO₂) concentrations from their pre-industrial value of 280 to 412 ppm in 2017, and concentrations of 850–1370 ppm are expected by the end of the century under the business-as-usual scenario RCP 8.5 (IPCC, 2013). The global ocean has already absorbed about 28 % of these anthropogenic CO₂ emissions (Le Quéré et al., 2015), leading to a global pH decrease of 0.11 units (Gattuso et al., 2015), a phenomenon known



as Ocean Acidification (OA). The surface ocean pH is expected to decrease by an additional 0.3–0.4 units under the RCP 8.5 scenario by 2100, and as much as 0.8 units by 2300 (Caldeira and Wickett, 2005; Doney et al., 2009; Feely et al., 2009). The accumulation of anthropogenic CO₂ in the atmosphere also results in an increase in the Earth's heat content that is primarily absorbed by the ocean (Wijffels et al., 2016), leading to an expected rise of sea surface temperatures of 3 to 5 °C by 2100 (IPCC, 2013). Whereas the effect of increasing atmospheric CO₂ partial pressures (pCO₂) on ocean chemistry is relatively well documented, the potential impacts of OA on marine organisms and how their response to OA will be modulated by the concurrent warming of the ocean surface waters are still the subject of much debate (Boyd and Hutchins, 2012; Gattuso et al., 2013).

Over the last decade, there has been increasing interest in the potential effects of OA on marine organisms (Kroeker et al., 2013). The first experiments were primarily conducted on single phytoplankton species (reviewed in Riebesell and Tortell, 2011), but subsequent mesocosm experiments highlighted the impact of OA on the structure and productivity of complex plankton assemblages (Riebesell et al., 2007, 2013). Due to their widely different initial and experimental conditions, these ecosystem-level experiments generated contrasting results (Schulz et al., 2017) but some general patterns nevertheless emerged. For example, diatoms generally benefit from higher pCO₂ through stimulated photosynthesis and growth rates since the increase in CO₂ concentrations compensates for the low affinity of RubisCO towards CO₂ (Giordano et al., 2005; Gao and Campbell, 2014). Although most phytoplankton species have developed carbon concentration mechanisms (CCM) to compensate for the low affinity of RubisCO towards CO₂, CCM efficiencies differ between taxa, rendering predictions of the impact of a CO₂ rise on the downregulation of CCM rather difficult (Raven et al., 2014). For example, some studies unexpectedly reported no significant or very modest stimulation of primary production under elevated CO₂ concentrations (Engel et al., 2005; Eberlein et al., 2017). OA can ultimately affect the structure of phytoplankton assemblages. Small cells such as photosynthetic picoeukaryotes can benefit directly from an increase in pCO₂ as CO₂ can passively diffuse through their boundary layer (Beardall et al., 2014), and the smallest organisms within this group could benefit most from the increase (Brussaard et al., 2013). Accordingly, OA experiments have typically favoured smaller phytoplankton cells (Yoshimura et al., 2010; Brussaard et al., 2013; Morán et al., 2015), although the proliferation of larger cells has also been reported (Tortell et al., 2002). Hence, generic predictions of phytoplankton community responses to OA are challenging.

Few recent studies have investigated the combined effects of OA and warming on natural phytoplankton assemblages (Hare et al., 2007; Feng et al., 2009; Maugendre et al., 2015; Paul et al., 2015, 2016). Laboratory experiments have shown that OA and warming could together increase photosynthetic rates, but at the expense of species richness, the reduction of diversity predominantly imputable to warming (Tatters et al., 2013). Results of an experiment conducted with a natural planktonic community from the Mediterranean Sea showed no effect of a combined warming and decrease in pH on primary production, but higher picocyanobacteria abundances were observed in the warmer treatment (Maugendre et al., 2015). Shipboard microcosm incubations conducted in the northern South China Sea displayed higher phytoplankton biomass, daytime primary productivity and dark community respiration under warmer conditions, but these positive responses were cancelled at low pH (Gao et al., 2017). In contrast, a mesocosm experiment carried out with a fall planktonic community from the western Baltic



Sea led to a decrease in phytoplankton biomass under warming, but combined warming and increased $p\text{CO}_2$ led to an increase in biomass (Sommer et al., 2015). Results from experiments where the impacts of $p\text{CO}_2$ and temperature are investigated individually may be misleading as multiple stressors can interact antagonistically or synergistically, sometimes in a nonlinear, unpredictable fashion (Todgham and Stillman, 2013; Boyd et al., 2015; Riebesell and Gattuso, 2015; Gunderson et al., 2016). The Lower St. Lawrence Estuary (LSLE) is a large (9350 km²) segment of the greater St. Lawrence Estuary (d'Anglejan, 1990). From June to September, the LSLE is characterized by a dynamic succession in the phytoplankton community, mostly driven by changes in light and nutrient availability through variations in the intensity of vertical mixing (Levasseur et al., 1984). The spring and fall blooms are mostly comprised of diatoms, with simultaneous nitrate and silicic acid exhaustion ultimately limiting primary production (Levasseur et al., 1987; Roy et al., 1996). How OA and warming may affect these blooms and primary production has never been investigated in the LSLE. The OA problem is complex in estuarine and coastal waters where freshwater runoff, tidal mixing, and high biological activity contribute to variations in $p\text{CO}_2$ and pH on different time scales (Duarte et al., 2013). The surface mixed-layer $p\text{CO}_2$ in the LSLE varies spatially from 139 to 548 μatm and is strongly modulated by biological productivity (Dinauer and Mucci, 2017). Surface pH_T has been shown to vary from 7.85 to 7.93 in a single tidal cycle in the LSLE, nearly as much as the world's oceans have experienced in response to anthropogenic CO_2 uptake over the last century (Caldeira and Wickett, 2005; Mucci et al., 2017).

The main objective of this study was to experimentally assess the sensitivity of the LSLE phytoplankton fall assemblage to a large $p\text{CO}_2$ gradient at two temperatures (in situ and +5 °C). Whether lower trophic-level microorganisms thriving in a highly variable environment will show higher resistance or resilience to future anthropogenic forcings is still a matter of speculation.

2. Material and methods

2.1 Mesocosm setup

The mesocosm system consists of two thermostated full-size ship containers each holding six 2600 L mesocosms (Aquabiotech®). The mesocosms are cylindrical with a cone-shaped bottom within which mixing is achieved using a propeller fixed near the top. Each enclosure is sealed with a Plexiglas cover allowing the transmission of 90 % of photosynthetically active radiation (PAR; 400–700 nm), 50–85 % of solar UVB (280–315 nm) and 85–90 % of UVA (315–400 nm). The mesocosms are equipped with individual, independent temperature probes (AQBT-Temperature sensor, accuracy ± 0.2 °C). Temperature in the mesocosms was measured every 15 minutes during the experiment, and the control system triggered either a resistance heater (Process Technology TTA1.8215) located near the middle of the mesocosm or a pump-activated glycol refrigeration system to maintain the set temperature. The pH in each mesocosm was monitored every 15 minutes using Hach® PD1P1 probes (± 0.02 pH units) connected to Hach® SC200 controllers, and positive deviations from the target values activated peristaltic pumps linked to a reservoir of artificial seawater equilibrated with pure CO_2 prior to the onset of the experiment. This system maintained the pH of the seawater in the mesocosms within ± 0.02 pH units of the targeted values by lowering



the pH during autotrophic growth but could not increase the pH during bloom senescence when the $p\text{CO}_2$ rose and pH decreased.

2.2 Setting

The water was collected at 5 m depth near Rimouski harbour ($48^\circ 28' 39.9''$ N, $68^\circ 31' 03.0''$ W) on the 27th of September 2014. In situ conditions were: salinity = 26.52, temperature = 10°C , nitrate (NO_3^-) = $12.8 \pm 0.6 \mu\text{mol L}^{-1}$, silicic acid (Si(OH)_4) = $16 \pm 2 \mu\text{mol L}^{-1}$, and soluble reactive phosphate (SRP) = $1.4 \pm 0.3 \mu\text{mol L}^{-1}$. The same day (indicated as day -5 hereafter), the water was filtered through a $250 \mu\text{m}$ mesh while simultaneously filling the 12 mesocosm tanks by gravity with a custom made ‘octopus’ tubing system. The initial in situ temperature of 10°C was maintained in the twelve mesocosms for the first 24 h (day -4). After that period, the six mesocosms in one container were maintained at 10°C while temperature was gradually increased to 15°C during day -3 in the six mesocosms of the other container. To avoid subjecting the planktonic communities to excessive stress due to sudden changes in temperature and pH while setting the experiment, the mesocosms were left to acclimatize on day -2 before acidification was carried out over day -1. One mesocosm from each temperature-controlled container was not pH-controlled to assess the community response to the freely fluctuating pH. These two mesocosms were labelled “Controls” as the initial in situ pH was allowed to fluctuate over time with the development of the phytoplankton bloom. The other mesocosms were set to cover a range of pH_T of ca. 8.0 to ca. 7.2 corresponding to a $p\text{CO}_2$ gradient of ca. 440 to ca. 2900 μatm after acidification was carried out.

2.3 Seawater analysis

The mesocosms were sampled between 05:00 and 08:00 a.m. every day. Seawater for carbonate chemistry, nutrients, and primary production were collected directly from the mesocosms as close to sunrise as possible. Seawater was also collected in 20 L carboys for the determination of chlorophyll *a* (Chl *a*), taxonomy, and other variables. Samples for salinity were taken from the artificial seawater tanks and in the mesocosms on day -3, 3 and 13. The samples were collected in 250 mL plastic bottles and stored in the dark until analysis was performed using a Guildline Autosol 8400B Salinometer during the following months.

2.3.1 Carbonate chemistry

Carbonate chemistry parameters were determined using methods described in Mucci et al. (2017). Briefly, water samples for pH (every day) and total alkalinity (TA, every 3–4 days) measurements were, respectively, transferred from the mesocosms to 125 mL plastic bottles without headspace and 250 mL glass bottles. A few crystals of HgCl_2 were added to the glass bottles before sealing them with a ground-glass stopper and Apiezon® Type-M high-vacuum grease. The pH was determined within hours of collection, after thermal equilibration at $25.0 \pm 0.1^\circ\text{C}$, using a Hewlett-Packard UV-Visible diode array spectrophotometer (HP-8453A) and a 5 cm quartz cell with phenol red (PR; Robert-Baldo et al., 1985) and *m*-cresol purple (mCP; Clayton and Byrne, 1993) as indicators. Measurements were carried out at the wavelength of maximum absorbance of



the protonated (HL) and deprotonated (L) indicators. Comparable measurements were carried out using a TRIS buffer prepared at a practical salinity of ca. 25 before and after each set of daily measurements (Millero, 1986). The pH on the total proton concentration scale (pH_T) of the buffer solutions and samples at 25 °C was calculated according to the equation of Byrne (1987), using the salinity of each sample and the HSO_4^- association constants given by Dickson (1990). The TA was determined on site within one day of sampling by open-cell automated potentiometric titration (Titralab 865, Radiometer®) with a pH combination electrode (pHC2001, Red Rod®) and a dilute (0.025N) HCl titrant solution. The titrant was calibrated using Certified Reference Materials (CRM Batch#94, provided by A. G. Dickson, Scripps Institute of Oceanography, La Jolla, USA). The average relative error, based on the average relative standard deviation on replicate standard and sample analyses, was better than 0.15 %. The carbonate chemistry parameters at in situ temperature were then calculated using the computed pH_T at 25 °C in combination with the measured TA using CO₂SYS (Pierrot et al., 2006) and the carbonic acid dissociation constants of Cai and Wang (1998).

2.3.3 Nutrients

Samples for NO_3^- , Si(OH)_4 , and SRP analyses were collected directly from the mesocosms every day, filtered through Whatman GF/F filters and stored at -20 °C in acid washed polyethylene tubes until analysis by a Bran and Luebbe Autoanalyzer III using the colorimetric methods described by Hansen and Koroleff (2007). The analytical detection limit was 0.03 $\mu\text{mol L}^{-1}$ for NO_3^- plus nitrite (NO_2^-), 0.02 $\mu\text{mol L}^{-1}$ for NO_2^- , 0.1 $\mu\text{mol L}^{-1}$ for Si(OH)_4 , and 0.05 $\mu\text{mol L}^{-1}$ for SRP.

2.3.4 Plankton biomass, composition and enumeration

Duplicate subsamples (100 mL) for Chl *a* determination were filtered onto Whatman GF/F filters. Chl *a* concentrations were measured using a 10-AU Turner Designs fluorometer, following a 24 h extraction in 90 % acetone at 4 °C in the dark without grinding (acidification method: Parsons et al., 1984). The analytical detection limit for Chl *a* was 0.05 $\mu\text{g L}^{-1}$.

Pico- (0.2–2 μm) and nanophytoplankton (2–20 μm) cell abundances were determined daily by flow cytometry. Sterile cryogenic polypropylene vials were filled with 4.95 mL of seawater to which 50 μL of glutaraldehyde Grade I (final concentration = 0.1 %, Sigma Aldrich; Marie et al., 2005) were added. Duplicate samples were flash frozen in liquid nitrogen after standing 15 minutes at room temperature in the dark. These samples were then stored at -80 °C until analysis. After thawing to ambient temperature, samples were analyzed using a FACS Calibur flow cytometer (Becton Dickinson) equipped with a 488 nm argon laser. The abundances of nanophytoplankton and picophytoplankton, which includes photosynthetic picoeukaryotes and picocyanobacteria, were determined by their autofluorescence characteristics and size (Marie et al., 2005). The biomass accumulation and nanophytoplankton growth rates were calculated by the following equation:

$$\mu = \ln(N_2/N_1) / (t_2 - t_1), \quad (1)$$

where N_1 and N_2 are the biomass or cell concentrations at given times t_1 and t_2 , respectively.



Microscopic identification and enumeration for eukaryotic cells larger than 2 μm was conducted on samples taken from each mesocosm on three days: day -4, the day when maximum Chl *a* was attained in each mesocosm, and day 13. Samples of 250 mL were collected and preserved with acidic Lugol solution (Parsons et al., 1984), then stored in the dark until analysis. Cell identification was carried out at the lowest possible taxonomic rank using an inverted microscope (Zeiss Axiovert 10) in accordance with Lund et al. (1958). The main taxonomic references used to identify the phytoplankton were Tomas (1997) and Bérard-Therriault et al. (1999).

2.3.5 Primary production

Primary production was determined daily using the ^{14}C -fixation incubation method (Knap et al., 1996; Ferland et al., 2011). One clear and one dark 250 mL polycarbonate bottle were filled from each mesocosm at dawn and spiked with 250 μL of $\text{NaH}^{14}\text{CO}_3$ (80 $\mu\text{Ci mL}^{-1}$). One hundred μL of 3-(3,4-dichlorophenyl)-1,1-dimethylurea (DCMU) (0.02 mol L^{-1}) was added to the dark bottles to prevent active fixation of ^{14}C by phytoplankton (Legendre et al., 1983). The total amount of radioisotope in each bottle was determined by immediately pipetting 50 μL subsamples into a 20 mL scintillation vial containing 10 mL of scintillation cocktail (EcolumeTM) and 50 μL of ethanolamine (Sigma). Bottles were placed in separate incubators, at either 10 °C or 15 °C, under reduced (30 %) natural light for 24 h, which corresponds to the light transmittance at mid-mesocosm depth.

At the end of the incubation periods, 3 mL were transferred to a scintillation vial for determination of the total primary production (P_T), 3 mL were filtered through a syringe filter (GD/X 0.7 μm) to estimate daily photosynthetic carbon fixation released in the dissolved organic carbon pool (P_D). The remaining volume was filtered onto a Whatman GF/F filter to measure the particulate primary production (P_P). Vials containing the P_T and P_D samples were acidified with 500 μL of HCl 6 N, allowed to sit for 3 h under a fume hood, then neutralized with 500 μL of NaOH 6 N. The vials containing the filters were acidified with 100 μL of 0.05 N HCl and left to fume for 12 h. Fifteen mL of scintillation cocktail were added to the vials and they were stored pending analysis using a Tri-Carb 4910TR liquid scintillation counter (PerkinElmer). Rates of carbon fixation into particulate and dissolved organic matter were calculated according to Knap et al. (1996) using the dissolved inorganic carbon concentration computed for each mesocosm at the beginning of the daily incubations and multiplied by a factor of 1.05 to correct for the lower uptake of ^{14}C compared to ^{12}C .

2.4 Statistical analysis

All statistical analyses were performed using R (nlme package). A general least squares (glms) model approach was used to test the linear effects of the two treatments (temperature, pCO_2), and of their interactions on the measured variables (Paul et al., 2016; Husserr et al., 2017). The analysis was conducted independently on two different time periods: Phase I (day 0 to day 4) corresponded to the development of the diatom bloom and extended up to the depletion of nitrate, whereas Phase II (day 5 to day 13) corresponded to the declining phase of the bloom in the absence of detectable nitrate. Averages (or time-integration in the case of primary production) of the response variables were calculated separately over the two phases and were plotted



against $p\text{CO}_2$. Separate regressions were performed with $p\text{CO}_2$ as the continuous factor for each temperature when a temperature effect or interaction with $p\text{CO}_2$ was detected in the gls model. Otherwise, the model included data from both temperatures and the interaction with $p\text{CO}_2$. Normality of the residuals was determined using a Shapiro-Wilk test ($p > 0.05$) and data were transformed (natural logarithm or square root) if required. As explained by Havenhand et al. (2010), the gradient approach, instead of treatment replication, is particularly suitable when few experimental units are available such as in large volume mesocosm experiments.

3. Results

3.1 Seawater chemistry

Water salinity was 26.52 ± 0.03 on day -4 in all mesocosms and remained constant throughout the experiment, averaging 26.54 ± 0.02 on day 13. The TA was practically invariant in the mesocosms, averaging $2057 \pm 2 \mu\text{mol kg}_{\text{sw}}^{-1}$ on day -4 and $2058 \pm 2 \mu\text{mol kg}_{\text{sw}}^{-1}$ on day 13. The pH remained relatively stable throughout the experiment in the pH-controlled treatments, but decreased slightly during Phase II by an average of -0.14 ± 0.07 units relative to the target pH_T (Fig. 1a). Given a constant TA, pH variations were accompanied by variations in $p\text{CO}_2$, from an average of $1340 \pm 150 \mu\text{atm}$ on day -3, and ranging from 564 to $2902 \mu\text{atm}$ at 10°C , and from 363 to $2884 \mu\text{atm}$ at 15°C on day 0 following the acidification (Fig. 1b). The pH_T in the Controls (M6 and M11) increased from 7.896 and 7.862 on day 0 at 10°C and 15°C , respectively, to 8.307 and 8.554 on day 13, reflecting the balance between CO_2 uptake and metabolic CO_2 production over the duration of the experiment. On the last day, $p\text{CO}_2$ in all mesocosms ranged from 186 to $3695 \mu\text{atm}$ at 10°C , and from 90 to $3480 \mu\text{atm}$ at 15°C . The temperature of the mesocosms in each container remained within $\pm 0.1^\circ\text{C}$ of the target temperature throughout the experiment and averaged $10.04 \pm 0.02^\circ\text{C}$ for mesocosms M1 through M6, and $15.0 \pm 0.1^\circ\text{C}$ for mesocosms M7 through M12 (Fig. 1c).

3.2 Dissolved inorganic nutrient concentrations

Nutrient concentrations averaged $9.1 \pm 0.5 \mu\text{mol L}^{-1}$ for NO_3^- , $13.4 \pm 0.3 \mu\text{mol L}^{-1}$ for $\text{Si}(\text{OH})_4$, and $0.91 \pm 0.03 \mu\text{mol L}^{-1}$ for SRP on day 0 (Fig. 1d, e, f). The three nutrients displayed a similar temporal depletion pattern following the development of the phytoplanktonic bloom. NO_3^- concentrations reached undetectable in all mesocosms on day 5. Likewise, $\text{Si}(\text{OH})_4$ fell below the detection limit between day 1 and 5 in all mesocosms except for those whose pH_T was set at 7.2 and 7.6 at 10°C (M5 and M3) and in which $\text{Si}(\text{OH})_4$ depletion occurred on day 9. Variations in SRP concentrations followed closely those of NO_3^- in all mesocosms except again for those set at pH 7.2 and 7.6 in which undetectable values were reached on day 9.

3.3 Phytoplankton biomass

Chl *a* concentrations were below $1 \mu\text{g L}^{-1}$ just after the filling of the mesocosms, and averaged $5.9 \pm 0.6 \mu\text{g L}^{-1}$ on day 0 (Fig. 2a). They then quickly increased to reach maximum concentrations around $27 \pm 2 \mu\text{g L}^{-1}$ on day 3 ± 2 , and decreased progressively until the end of the experiment. During Phase I, results from the gls model show no significant relationships



between the mean Chl *a* concentrations and pCO₂ at the two temperatures tested but significantly higher Chl *a* values at 15 °C than at 10 °C (Fig. 2b; Table 1). During this phase, the accumulation rate of Chl *a* was positively affected by temperature, but not by the pCO₂ gradient (Fig. 3a; Table 2). The maximum Chl *a* concentrations reached during the bloom were not affected by the two treatments (Fig. 3b; Table 2). During Phase II, we observed no significant effect of increasing pCO₂ on the mean Chl *a* concentrations at the two temperatures tested. Nevertheless, during that phase, the mean Chl *a* concentrations decreased from $18.2 \pm 0.9 \mu\text{g L}^{-1}$ at 10 °C to $12.4 \pm 0.7 \mu\text{g L}^{-1}$ at 15 °C, suggesting a faster loss of the pigments following the depletion of NO₃⁻.

3.4 Phytoplankton size-class

Nanophytoplankton abundance varied from $8 \pm 1 \times 10^6 \text{ cells L}^{-1}$ on day 0 to an average maximum of $36 \pm 10 \times 10^6 \text{ cells L}^{-1}$ at the peak of the bloom (Fig. 2d). At both temperatures, nanophytoplankton abundance increased until at least days 2 or 4 and decreased or remained stable thereafter. The strong correlation between the nanophytoplankton abundance and Chl *a* ($r^2 = 0.82$, $p < 0.001$) suggests that this phytoplankton size class was responsible for most of the biomass build-up in the mesocosms. As observed for the mean Chl *a* concentration, the mean abundance of nanophytoplankton was not significantly affected by the pCO₂ gradient at the two temperatures investigated during Phase I, but showed higher values at 15 °C ($31 \pm 3 \times 10^6 \text{ cells L}^{-1}$) than at 10 °C ($13 \pm 2 \times 10^6 \text{ cells L}^{-1}$) (Fig. 2e; Table 1). Likewise, the growth rate of nanophytoplankton during Phase I was not influenced by the pCO₂ gradient at the two temperatures but was significantly higher in the warm treatment (Fig. 3c; Table 2). During Phase II, no relationship was found between the mean nanophytoplankton abundance and the pCO₂ gradient at the two temperatures and no temperature effect was observed (Fig. 2f; Table 3).

Initial abundance of photosynthetic picoeukaryotes was $10 \pm 2 \times 10^6 \text{ cells L}^{-1}$, accounting for more than 80 % of total plankton cells in the 0.2–20 μm size fraction. The abundance of this plankton size fraction decreased slightly through Phase I and their number remained relatively stable at $3.3 \pm 0.2 \times 10^6 \text{ cells L}^{-1}$ throughout Phase II (Fig. 2g). We found no relationship between the abundance of picoeukaryotes and the pCO₂ gradient at the two temperatures investigated during both Phases I and II, and no temperature effect was observed either (Fig. 2h, i; Tables 1 and 3).

Picocyanobacteria exhibited a different pattern than the nanophytoplankton and picoeukaryotes (Fig. 2j). Their abundance was initially low ($1.7 \pm 0.3 \times 10^6 \text{ cells L}^{-1}$ on day 0), remained relatively stable during Phase I, and increased rapidly during Phase II, accounting for ca. 50 % of the total picophytoplankton cell counts toward the end of the experiment. During Phase I, the mean picocyanobacteria abundance was not influenced by the pCO₂ gradient but was higher at 15 °C ($1.4 \pm 0.2 \times 10^6 \text{ cells L}^{-1}$) than at 10 °C ($0.95 \pm 0.05 \times 10^6 \text{ cells L}^{-1}$) (Fig. 2k; Table 1). During Phase II, their mean abundance remained higher at 15 °C ($4.5 \pm 0.3 \times 10^6 \text{ cells L}^{-1}$) than at 10 °C ($2.6 \pm 0.1 \times 10^6 \text{ cells L}^{-1}$), and again no significant effect of pCO₂ was detected (Fig. 2l; Table 3).



3.5 Phytoplankton taxonomy

The taxonomic composition of the planktonic assemblage larger than 2 μm was identical in all treatments at the beginning of the experiment, and was mainly composed of the cosmopolitan chain-forming centric diatom *Skeletonema costatum* (*S. costatum*) and the cryptophyte *Plagioselmis prolunga* var. *nordica* (Fig. 4). At the peak of the blooms (maximum Chl *a* concentrations), the species composition did not vary between the pCO_2 treatments and between the two temperatures tested. *S. costatum* was the dominant species in all mesocosms (70–90 % of the total number of eukaryotic cells), except for one mesocosm (M3, pH 7.6 at 10 °C) where a mixed dominance of *Chrysochromulina* spp. (a prymnesiophyte of 2–5 μm) and *S. costatum* was observed (Fig. 4a). *S. costatum* accounted for 80–90 % of the total eukaryotic cell counts in all mesocosms at the end of the experiment carried out at 10 °C. At 15 °C, the composition of the assemblage had shifted toward a dominance of unidentified flagellates and choanoflagellates (2–20 μm) in all mesocosms with these two groups accounting for 55–80 % of the total cell counts while diatoms showed signs of loss of viability as indicated by the presence of empty frustules (Fig. 4b).

3.6 Primary production

P_P increased in all mesocosms during Phase I of the experiment, in parallel with the increase in Chl *a* (Fig. 5a). P_P maxima were attained on days 3–4, except for the 15 °C Control (M11) where P_P peaked on day 1. We found no significant effect of the pCO_2 gradient on the time-integrated P_P at the two temperatures during both Phases I and II (Fig. 5b, c; Tables 1 and 3), but time-integrated P_P was higher at 15 °C than at 10 °C during Phase I and lower at 15 °C than at 10 °C during Phase II (Tables 1 and 3). Similar opposite responses to warming were observed when normalizing P_P per unit of Chl *a* (Fig. 5g, h, i). Initial Chl *a*-normalized P_P values were $3.3 \pm 0.5 \mu\text{mol C} (\mu\text{g Chl } a)^{-1} \text{ d}^{-1}$ and reached maxima between $3.7 \pm 0.3 \mu\text{mol C} (\mu\text{g Chl } a)^{-1} \text{ d}^{-1}$ and $6.0 \pm 0.7 \mu\text{mol C} (\mu\text{g Chl } a)^{-1} \text{ d}^{-1}$ at 10 °C and 15 °C, respectively. These values then decreased to $2.2 \pm 0.6 \mu\text{mol C} (\mu\text{g Chl } a)^{-1} \text{ d}^{-1}$ and $0.9 \pm 0.2 \mu\text{mol C} (\mu\text{g Chl } a)^{-1} \text{ d}^{-1}$ on the last day of the experiment (Fig. 5g). During Phase I, the mean Chl *a*-normalized P_P was significantly higher under warming, but as observed for Chl *a* concentrations and P_P , was not affected by the pCO_2 gradient (Fig. 5h; Table 1). During Phase II, the mean Chl *a*-normalized P_P decreased with increasing temperature, with values of $2.2 \pm 0.2 \mu\text{mol C} (\mu\text{g Chl } a)^{-1} \text{ d}^{-1}$ and $1.6 \pm 0.1 \mu\text{mol C} (\mu\text{g Chl } a)^{-1} \text{ d}^{-1}$ at 10 °C and 15 °C, respectively (Fig. 5i; Table 3). No significant effect of pCO_2 was detected.

P_D was low at the beginning of the experiment, averaging $1.5 \pm 0.4 \mu\text{mol C L}^{-1} \text{ d}^{-1}$, increased progressively during Phase I to reach values of up to $48 \mu\text{mol C L}^{-1} \text{ d}^{-1}$ on days 4 and 5 at the beginning of Phase II, and decreased thereafter (Fig. 5d). Time-integrated P_D was affected neither by the pCO_2 gradient at the two temperatures tested nor by temperature during the two Phases (Fig. 5e, f; Tables 1 and 3). Chl *a*-normalized P_D was low on day 0, averaging $0.3 \pm 0.1 \mu\text{mol C} (\mu\text{g Chl } a)^{-1} \text{ d}^{-1}$, reached maximum values of $1.4 \pm 0.5 \mu\text{mol C} (\mu\text{g Chl } a)^{-1} \text{ d}^{-1}$ at the beginning of Phase II, and decreased to $0.3 \pm 0.4 \mu\text{mol C} (\mu\text{g Chl } a)^{-1} \text{ d}^{-1}$ by the end of the experiment (Fig. 5j). During Phases I and II, the mean Chl *a*-normalized P_D



were affected neither by the temperature and pCO₂ gradient, nor by the interaction between those factors (Fig. 5k, l; Tables 1 and 3).

Figure 6 shows the influence of the treatments on maximum P_P and P_D as well as on the time-integrated P_P and P_D over the full length of the experiment. We found no effect of the pCO₂ gradient on the maximum P_P values at the two temperatures tested, but warming increased the maximum P_P values from $66 \pm 13 \mu\text{mol C L}^{-1} \text{d}^{-1}$ to $126 \pm 8 \mu\text{mol C L}^{-1} \text{d}^{-1}$ (Fig. 6a; Table 4). The time-integrated P_P over the full duration of the experiment was not affected by the pCO₂ gradient or the increase in temperature (Fig. 6b; Table 4). The absence of temperature effect results from the countervailing responses in time-integrated P_P between Phases I and II. The maximum P_D values were significantly affected by the treatments (Fig 6c; Table 4). Maximum P_D decreased with increasing pCO₂ at in situ temperature but warming cancelled this effect (antagonistic effect). Nevertheless, the time-integrated P_D over the whole experiment did not vary significantly between treatments, although a decreasing tendency with increasing pCO₂ at 10 °C and an increasing tendency with warming can be seen in Fig. 6d (Table 4).

4. Discussion

4.1 General characteristics of the bloom

A phytoplankton bloom, numerically dominated by the centric diatom *S. costatum*, took place in all mesocosms, regardless of treatments (Fig. 4). *S. costatum* is a common phytoplankton species in the St. Lawrence Estuary and in coastal waters (Kim et al., 2004; Starr et al., 2004; Annane et al., 2015). The length of the experiment (13 days) allowed us to capture both the development and declining phases of the bloom. The exponential growth phases lasted 1–4 days depending on the treatments, but maximal Chl *a* concentrations were reached only after 7 days in two of the twelve mesocosms (Fig. 2a). The suite of measurements and statistical tests conducted did not provide any clues as to the underlying causes for the lower rates of biomass accumulation measured in these two mesocosms. Since statistical analyses conducted with or without these two apparent outliers gave similar results, they were not excluded from the analyses.

During the development phase of the bloom, the concentration of all three monitored nutrients decreased, with NO₃⁻ and Si(OH)₄ reaching undetectable values. This nutrient co-depletion is consistent with results from previous studies suggesting a co-limitation of diatom blooms by these two nutrients in the St. Lawrence Estuary (Levasseur et al., 1987, 1990). Variations in P_P roughly followed changes in Chl *a*, and, as expected, the maximum Chl *a*-normalized P_P ($5 \pm 2 \mu\text{mol C} (\mu\text{g Chl } a)^{-1} \text{d}^{-1}$) was reached during the exponential growth phase in all mesocosms. Decreases in total phytoplankton abundances and P_P followed the bloom peaks and the timing of the NO₃⁻ and Si(OH)₄ depletions. A clear succession in phytoplankton size classes characterized the experiment. Nanophytoplankton cells were initially present in low abundance and became more numerous as the *S. costatum* diatom bloom developed. The strong correlation ($r^2 = 0.83$, $p < 0.001$) between the abundance of nanophytoplankton and *S. costatum* enumeration suggests that this cell size class can be used as a proxy of *S. costatum* counts in all mesocosms throughout the experiment. Nanophytoplankton cells accounted for $79 \pm 7 \%$ of total counts of cells $< 20 \mu\text{m}$ on the day of the maximum Chl *a* concentration. Accordingly, nanophytoplankton exhibited the same temporal trend as Chl *a*



concentrations. During Phase II, nanophytoplankton abundances remained roughly stable at in situ temperature but decreased at 15 °C. Photosynthetic picoeukaryotes were originally abundant and decreased throughout the experiment whereas picocyanobacteria abundances increased during Phase II. This is a typical phytoplankton succession pattern for temperate systems where an initial diatom bloom growing essentially on allochthonous nitrate gives way to smaller species growing on regenerated forms of nitrogen (Taylor et al., 1993).

4.2 Phase I (Diatom bloom development)

Our results show no significant effect of increasing pCO₂/decreasing pH on the mean abundance and net accumulation rate of the diatom-dominated nanophytoplankton assemblage during the development of the bloom (Figs. 2e and 3c). These results suggest that *S. costatum*, the species accounting for most of the biomass accumulation during the bloom, neither benefited from the higher pCO₂ nor was negatively impacted by the lowering of pH. Assuming that *S. costatum* was also responsible for most of the carbon fixation during the bloom development phase, the absence of effect on P_p and Chl *a*-normalized P_p following increases in pCO₂ brings additional support to our conclusion. *S. costatum* operates a highly efficient CCM, minimizing the potential benefits of thriving in high CO₂ waters (Trimborn et al., 2009). This may explain why the strain present in the LSLE did not benefit from the higher pCO₂ conditions. Likewise, a mesocosm experiment conducted in the coastal North Sea showed no significant effect of increasing pCO₂ on carbon fixation during the development of the spring diatom bloom (Bach et al., 2017; Eberlein et al., 2017).

In addition to the aforementioned insensitivity to increasing pCO₂, our results point towards a strong resistance of *S. costatum* to severe pH decline. During our study, surprisingly constant rates of Chl *a* accumulation and nanophytoplankton growth (Fig. 3a, c), as well as maximum P_p (Fig. 6a), were measured during the development phase of the bloom over a range of pH_T extending from 8.6 to 7.2 (Fig. 1a). In a recent effort to estimate the causes and amplitudes of short-term variations in pH_T in the LSLE, Mucci et al. (2017) showed that pH_T in surface waters was constrained within a range of 7.85 to 7.93 during a 50-h survey over two tidal cycles at the head of the Laurentian Channel. It is notable that even the upwelling of water from 100 m depth or of low-oxygen LSLE bottom water would not decrease pH_T beyond ca. 7.75 and 7.62, respectively (Mucci et al., 2017 and references therein). Our results show that the phytoplankton assemblage responsible for the fall bloom may tolerate even greater pH_T excursions. In the LSLE, such conditions may arise when the contribution of the low pH_T (7.12) freshwaters of the Saguenay River to the LSLE surface waters is amplified during the spring freshet. However, considering that comparable studies conducted in different environments have reported negative effects of decreasing pH on diatom biomass accumulation (Hare et al., 2007; Hopkins et al., 2010; Schulz et al., 2013), it cannot be concluded that all diatom species thriving in the LSLE are insensitive to acidification.

In contrast to the pCO₂ treatment, warming affected the development of the bloom in several ways. Increasing temperature by 5 °C significantly increased the accumulation rate of Chl *a*, the nanophytoplankton growth rate, as well as the time-integrated P_p and Chl *a*-normalized P_p during Phase I of the bloom. The positive effects of warming on the Chl *a*-normalized P_p during the development phase of the bloom most likely reflect the sensitivity of photosynthesis to temperature (Sommer and



Lengfellner, 2008; Kim et al., 2013). It could also be related to optimal growth temperatures, which are often higher than in situ temperatures in marine phytoplankton (Thomas et al., 2012; Boyd et al., 2013). In support of this hypothesis, previous studies have reported optimal growth temperatures of 20–25 °C for *S. costatum*, which is 5–10 °C higher than the warmer treatment investigated in our study (Suzuki and Takahashi, 1995; Montagnes and Franklin, 2001). Extrapolating results from a mesocosm experiment to the field is not straightforward, as little is known of the projected warming of the upper waters of the LSLE in the next decades. In the Gulf of St. Lawrence, positive temperature anomalies in surface waters have varied from 0.25 to 0.75 °C per decade between 1985 and 2013 (Larouche and Galbraith, 2016). In the LSLE, warming of surface waters will likely result from a complex interplay between heat transfer at the air-water interface and variations in vertical mixing and upwelling of the cold intermediate layer at the head of the Estuary (Galbraith et al., 2014). Considering current uncertainties regarding future warming of the LSLE, studies should be conducted over a wider range of temperatures in order to better constrain the potential effect of warming on the development of the blooms in the LSLE.

Picoeukaryotes showed a more or less gradual decrease in abundance during Phase I, and our results show that this decline was not influenced by the increases in pCO₂ (Fig. 2g; Table 1). Picoeukaryotes are expected to benefit from high pCO₂ conditions even more so than diatoms as CO₂ can passively diffuse through their relatively thin boundary layer precluding the necessity of a costly uptake mechanism such as a CCM (Schulz et al., 2013). This hypothesis has been supported by several studies showing a stimulating effect of pCO₂ on picoeukaryote growth (Bach et al., 2016; Hama et al., 2016; Schulz et al., 2017 and references therein). On the other hand, in nature, the abundance of picoeukaryotes generally results from a delicate balance between cell division rates and cell losses through microzooplankton grazing and viral attacks. The few experiments, including the current study, reporting the absence or a modest effect of increasing pCO₂ on the abundance of eukaryotic picoplankton attribute their observations to an increase in nano- and microzooplankton grazing (Rose et al., 2009; Neale et al., 2014). During our experiment, the biomass of microzooplankton increased with increasing pCO₂ by ca. 200–300 % at the two temperatures tested (Ferreyra and Lemli, unpubl. data). Thus, it is possible that a positive effect of increasing pCO₂ and warming on picoeukaryote abundances might have been masked by higher picoeukaryote losses due to increased microzooplankton grazing.

4.3 Phase II (declining phase of the bloom)

The gradual decrease in nanophytoplankton abundances coincided with an increase in the abundance of picocyanobacteria (Fig. 2j). Regardless of temperature, the picocyanobacteria abundance during Phase II was unaffected by the increase in pCO₂ over the full range investigated (Fig. 2l; Table 3). The lack of positive response of picocyanobacteria to elevated pCO₂ was somewhat surprising considering that they have less efficient CCMs than diatoms (Schulz et al., 2013). Accordingly, several studies have reported a stimulation of the net growth rate of picocyanobacteria under elevated pCO₂ in different environments (coastal Japan, Mediterranean Sea, and Raunefjorden in Norway) and under different nutrient regimes, i.e. bloom and post-bloom conditions (Hama et al., 2016; Sala et al., 2016; Schulz et al., 2017). Consistent with our observations, however, Law et al. (2012) and Lomas et al. (2012) observed no direct effect of elevated pCO₂ on the net growth of picocyanobacteria during



studies conducted in the Subtropical North Atlantic and the South Pacific. In our study, a potential increase in grazing pressure, following the rise in heterotrophic nanoflagellates abundance (e.g. choanoflagellates; Fig. 4b) measured under high $p\text{CO}_2$ and warmer conditions, could explain the ostensible absence of stimulation of picocyanobacteria by increasing $p\text{CO}_2$. Despite the absence of grazing measurements during our study, our results support the hypothesis that the potential for increased picocyanobacteria population growth under elevated $p\text{CO}_2$ and temperature is partially dependent on different grazing pressures (Fu et al., 2007).

Warming, not acidification, affected carbon fixation during the declining phase of the bloom. In our study, the time-integrated primary production and Chl *a*-normalized primary production were not significantly affected by the increase in $p\text{CO}_2$ during Phase II at the two temperatures tested (Fig. 5, Table 3). This result is surprising since nitrogen-limited cells have been shown to be more sensitive to acidification, resulting in a reduction in carbon fixation rates due to higher respiration (Wu et al., 2010; Gao and Campbell, 2014; Raven et al., 2014). Although our measurements do not allow to discriminate between the contributions of the different phytoplankton size classes to carbon fixation, we can speculate that diatoms, which were still abundant during Phase II, contributed to a significant fraction of the primary production. If so, these results suggest that *S. costatum* remained insensitive to OA even under nutrient stress. However, in contrast to Phase I, increasing the temperature by 5 °C during Phase II significantly reduced P_p and the Chl *a*-normalized P_p . Dark phytoplankton respiration rates generally increase with temperature (Butrón et al., 2009; Robarts and Zohary, 1987). The warming-induced decrease in carbon fixation measured during Phase II may thus result from an increase in respiration by the nitrogen-limited diatoms.

4.4 Effect of the treatments on primary production over the full experiment

As mentioned above, increasing $p\text{CO}_2$ had no effect on time-integrated P_p during the two phases of the bloom, but warming resulted respectively in a positive and negative effect during Phases I and II. As a result, primary production rates integrated over the whole duration of the experiment were not significantly different between the two temperatures tested. Although not statistically significant, the time-integrated P_D s over the full experiment display a slight decrease with increasing $p\text{CO}_2$ at 10 °C and overall higher values in the warmer treatment (Fig. 6d; Table 4). Previous studies have reported increases of dissolved organic carbon (DOC) exudation (Engel et al., 2013), but also decreasing DOC concentrations at elevated $p\text{CO}_2$ under nitrate limitation (Yoshimura et al., 2014). The increase in DOC exudation is attributed to a stimulation of photosynthesis resulting from its sensitivity to higher $p\text{CO}_2$ (Engel et al. 2013), but the causes for a decrease in DOC concentrations at high $p\text{CO}_2$ are less clear and potentially attributable to an increase in transparent exopolymer particle (TEP) production (Yoshimura et al., 2014). Elevated TEP production under high $p\text{CO}_2$ conditions has been measured both at the peak of a bloom in a mesocosm study (Engel et al., 2014), and in post-bloom nutrient depleted conditions (MacGilchrist et al., 2014). However, during our study, TEP production decreased under high $p\text{CO}_2$ (Gaaloul, 2017). Thus, the apparent decrease in P_D cannot be attributed to a greater conversion of exuded dissolved carbohydrate into TEP. The apparent rise in P_D under warming is consistent with previous studies reporting similar increases in phytoplankton dissolved carbon release with temperature (Morán et al., 2006; Engel et al., 2011). Although these apparent changes in P_D with increasing $p\text{CO}_2$ and warming require further investigations,



they suggest that a larger proportion (ca. 15 % of P_T at 15 °C compared to 10 % at 10 °C) of the newly fixed carbon could be exuded and become available for heterotrophic organisms under warmer conditions.

5. Conclusion

Our results reveal a remarkable resistance of the different phytoplankton size classes to the large range of pCO_2 /pH investigated during our study. It is noteworthy that the plankton assemblage was submitted to decreases in pH far exceeding those that they are regularly exposed to in the LSLE. The resistance of *S. costatum* to the pCO_2 treatments suggests that the acidification of surface waters of the LSLE will not affect the development rate and the amplitude of fall blooms dominated by this species. Photosynthetic picoeukaryotes and picocyanobacteria thriving alongside the blooming diatoms were also insensitive to acidification. In contrast to the pCO_2 treatments, warming the water by 5 °C had multiple impacts on the development and decline of the bloom. The 5 °C warming hastened the development of the diatom bloom (albeit with no increase in total cells number) and increased the abundance of picocyanobacteria. These temperature-induced variations in the phytoplankton assemblage were accompanied, respectively, by higher then lower P_P during the development and declining phases of the diatom bloom. Due to these contrasting responses, warming had no net effect on P_P over the full temporal scale of the experiment. Overall, our results indicate that warming could have more important impacts than acidification on phytoplankton bloom development in the LSLE in the next decades. Future studies should be conducted and specifically designed to better constrain the potential effects of warming on phytoplankton succession and primary production in the LSLE.

Data availability. The data have been submitted to be freely accessible via <https://issues.pangaea.de/browse/PDI-16607>, or can be obtained by contacting the author (robin.benard.1@ulaval.ca).

Author contributions. R. Bénard was responsible for the experimental design elaboration, data sampling and processing, and the redaction of this article. Several co-authors supplied specific data included in this article, and all co-authors contributed to this final version of the article.

Competing interests. The authors declare that they have no conflict of interest.

Acknowledgements

The authors wish to thank the Station Aquicole ISMER, especially Nathalie Morin and her staff, for their support during the project. We also wish to acknowledge Gilles Desmeules, Bruno Cayouette, Sylvain Blondeau, Claire Lix, Rachel Husherr, Liliane St-Amand, Marjolaine Blais, Armelle Simo and Sonia Michaud for their help in setting up, sampling and processing samples during the experiment. The authors want to thank Jean-Pierre Gattuso for his constructive comments on an earlier draft of this manuscript. This study was funded by a Team grant from the Fonds de la Recherche du Québec – Nature et Technologies (FRQNT-Équipe-165335), the Canada Foundation for Innovation, and the Canada Research Chair on Ocean Biogeochemistry and Climate. This is a contribution to the research programme of Québec-Océan.



References

- Annane, S., St-Amand, L., Starr, M., Pelletier, E., and Ferreyra, G. A.: Contribution of transparent exopolymeric particles (TEP) to estuarine particulate organic carbon pool, *Mar. Ecol. Prog. Ser.*, 529, 17–34, doi:10.3354/meps11294, 2015.
- Bach, L. T., Taucher, J., Boxhammer, T., Ludwig, A., Aberle-Malzahn, N., Abrahamsson, K., Almén, A. K., Asplund, M. E., Audritz, S., Boersma, M., Breitbarth, E., Bridges, C., Brussaard, C., Brutemark, A., Clemmesen, C., Collins, S., Crawford, K., Dahlke, F., Deckelnick, M., Dittmar, T., Doose, R., Dupont, S., Eberlein, T., Endres, S., Engel, A., Engström-Öst, J., Febiri, S., Fleischer, D., Fritsche, P., Gledhill, M., Göttler, G., Granberg, M., Grossart, H. P., Grifos, A., Hoffmann, L., Karlsson, A., Klages, M., John, U., Jutfelt, F., Köster, I., Lange, J., Leo, E., Lischka, S., Lohbeck, K., Lundve, B., Mark, F. C., Meyerhöfer, M., Nicolai, M., Pansch, C., Petersson, B., Reusch, T., De Moraes, K. R., Schartau, M., Scheinin, M., Schulz, K. G., Schwarz, U., Stenegren, M., Stiasny, M., Storch, D., Stühr, A., Sswat, L., Svensson, M., Thor, P., Voss, M., Van De Waal, D., Wannicke, N., Wohlrab, S., Wulff, A., Achterberg, E. P., Algueró-Muñiz, M., Anderson, L. G., Bellworthy, J., Büdenbender, J., Czerny, J., Ericson, Y., Esposito, M., Fischer, M., Haunost, M., Hellemann, D., Horn, H. G., Hornick, T., Meyer, J., Sswat, M., Zark, M., and Riebesell, U.: Influence of ocean acidification on a natural winter-to-summer plankton succession: First insights from a long-term mesocosm study draw attention to periods of low nutrient concentrations, *PLoS ONE*, 11(8), 1–33, doi:10.1371/journal.pone.0159068, 2016.
- Bach, L. T., Alvarez-Fernandez, S., Hornick, T., Stühr, A., and Riebesell, U.: Simulated ocean acidification reveals winners and losers in coastal phytoplankton, *PLoS ONE*, 12(11), 1–22, doi:10.1371/journal.pone.0188198, 2017.
- Beardall, J., Stojkovic, S., and Gao, K.: Interactive effects of nutrient supply and other environmental factors on the sensitivity of marine primary producers to ultraviolet radiation: Implications for the impacts of global change, *Aquat. Biol.*, 22, 5–23, doi:10.3354/ab00582, 2014.
- Bérard-Therriault, L., Poulin, M., and Bossé, L.: Guide d'identification du phytoplancton marin de l'estuaire et du golfe du Saint-Laurent incluant également certains protozoaires., Canadian Special Publication of Fisheries and Aquatic Sciences, 128, 1–387, doi:10.1139/9780660960579, 1999.
- Boyd, P. W., and Hutchins, D. A.: Understanding the responses of ocean biota to a complex matrix of cumulative anthropogenic change, *Mar. Ecol. Prog. Ser.*, 470, 125–135, doi:10.3354/meps10121, 2012.
- Boyd, P. W., Rynearson, T. A., Armstrong, E. A., Fu, F., Hayashi, K., Hu, Z., Hutchins, D. A., Kudela, R. M., Litchman, E., Mulholland, M. R., Passow, U., Strzepek, R. F., Whittaker, K. A., Yu, E., and Thomas, M. K.: Marine Phytoplankton temperature versus growth responses from polar to tropical waters - outcome of a scientific community-wide study, *PLoS ONE*, 8(5), doi:10.1371/journal.pone.0063091, 2013.
- Boyd, P. W., Lennartz, S. T., Glover, D. M., and Doney, S. C.: Biological ramifications of climate-change-mediated oceanic multi-stressors, *Nat. Clim. Chang.*, 5(1), 71–79, doi:10.1038/nclimate2441, 2015.



- 473 Brussaard, C. P. D., Noordeloos, A. A. M., Witte, H., Collenteur, M. C. J., Schulz, K., Ludwig, A., and Riebesell, U.: Arctic
474 microbial community dynamics influenced by elevated CO₂ levels, *Biogeosciences*, 10(2), 719–731, doi:10.5194/bg-10-719-
475 2013, 2013.
- 476 Butrón, A., Iriarte, A., and Madariaga, I.: Size-fractionated phytoplankton biomass, primary production and respiration in the
477 Nervión-Ibaizabal estuary: A comparison with other nearshore coastal and estuarine ecosystems from the Bay of Biscay, *Cont.*
478 *Shelf Res.*, 29(8), 1088–1102, doi:10.1016/j.csr.2008.11.013, 2009.
- 479 Byrne, R. H.: Standardization of Standard Buffers by Visible Spectrometry, *Anal. Chem.*, 59, 1479–1481,
480 doi:10.1021/ac00137a025, 1987.
- 481 Cai, W. J., and Wang, Y.: The chemistry, fluxes, and sources of carbon dioxide in the estuarine waters of the Satilla and
482 Altamaha Rivers, Georgia, *Limnol. Oceanogr.*, 43(4), 657–668, doi:10.4319/lo.1998.43.4.0657, 1998.
- 483 Caldeira, K., and Wickett, M. E.: Ocean model predictions of chemistry changes from carbon dioxide emissions to the
484 atmosphere and ocean, *J. Geophys. Res.*, 110(C9), 1–12, doi:10.1029/2004JC002671, 2005.
- 485 Clayton, T. D., and Byrne, R. H.: Spectrophotometric seawater pH measurements: total hydrogen ion concentration scale
486 calibration of m-cresol purple and at-sea results, *Deep. Res. Part I*, 40(10), 2115–2129, doi:10.1016/0967-0637(93)90048-8,
487 1993.
- 488 d'Anglejan, B.: Recent sediments and sediment transport processes in the St. Lawrence Estuary, in: *Oceanography of a large-*
489 *scale estuarine system*, Eds: El-Sabh, M. I., and Silverberg, N., Springer-Verlag, New York, USA, 109–129, doi:
490 10.1002/9781118663783.ch6, 1990.
- 491 Dickson, A. G.: Standard potential of the reaction: $\text{AgCl(s)} + 1/2\text{H}_2\text{(g)} = \text{Ag(s)} + \text{HCl(aq)}$ and the standard acidity constant of
492 the ion HSO_4^- in synthetic sea water from 273.15 to 318.15 K, *J. Chem. Thermodyn.*, 22(2), 113–127, doi:10.1016/0021-
493 9614(90)90074-Z, 1990.
- 494 Dinauer, A., and Mucci, A.: Spatial variability in surface-water pCO₂ and gas exchange in the world's largest semi-enclosed
495 estuarine system: St. Lawrence Estuary (Canada), *Biogeosciences*, 14(13), 3221–3237, doi:10.5194/bg-14-3221-2017, 2017.
- 496 Doney, S. C., Fabry, V. J., Feely, R. A., and Kleypas, J. A.: Ocean acidification: The other CO₂ problem, *Ann. Rev. Mar. Sci.*,
497 1(1), 169–192, doi:10.1146/annurev.marine.010908.163834, 2009.
- 498 Duarte, C. M., Hendriks, I. E., Moore, T. S., Olsen, Y. S., Steckbauer, A., Ramajo, L., Carstensen, J., Trotter, J. A., and
499 McCulloch, M.: Is ocean acidification an open-ocean syndrome? Understanding anthropogenic impacts on seawater pH,
500 *Estuaries Coasts*, 36(2), 221–236, doi:10.1007/s12237-013-9594-3, 2013.
- 501 Eberlein, T., Wohrlab, S., Rost, B., John, U., Bach, L. T., Riebesell, U., and Van De Waal, D. B.: Effects of ocean acidification
502 on primary production in a coastal North Sea phytoplankton community, *PLoS ONE*, 12(3), e0172594,
503 doi:10.1371/journal.pone.0172594, 2017.
- 504 Engel, A., Zondervan, I., Aerts, K., Beaufort, L., Benthien, A., Chou, L., Delille, B., Gattuso, J.-P., Harlay, J., Heeman, C.,
505 Hoffmann, L., Jacquet, S., Nejstgaard, J., Pizay, M.-D., Rochelle-Newall, E., Schneider, U., Terbrueggen A., and Riebesell,



- 506 U.: Testing the direct effect of CO₂ concentration on a bloom of the coccolithophorid *Emiliania huxleyi* in mesocosm
507 experiments, *Limnol. Oceanogr.*, 50(2), 493–507, doi:10.4319/lo.2005.50.2.0493, 2005.
- 508 Engel, A., Händel, N., Wohlers, J., Lunau, M., Grossart, H.-P., Sommer, U., and Riebesell, U.: Effects of sea surface warming
509 on the production and composition of dissolved organic matter during phytoplankton blooms: Results from a mesocosm study,
510 *J. Plankton Res.*, 33(3), 357–372, doi:10.1093/plankt/fbq122, 2011.
- 511 Engel, A., Borchard, C., Piontek, J., Schulz, K. G., Riebesell, U., and Bellerby, R.: CO₂ increases ¹⁴C primary production in
512 an Arctic plankton community, *Biogeosciences*, 10(3), 1291–1308, doi:10.5194/bg-10-1291-2013, 2013.
- 513 Engel, A., Piontek, J., Grossart, H.-P., Riebesell, U., Schulz, K. G., and Sperling, M.: Impact of CO₂ enrichment on organic
514 matter dynamics during nutrient induced coastal phytoplankton blooms, *J. Plankton Res.*, 36(3), 641–657,
515 doi:10.1093/plankt/fbt125, 2014.
- 516 Feely, R. A., Doney, S. C., and Cooley, S. R.: Ocean acidification: present conditions and future changes in a high-CO₂ world,
517 *Oceanography*, 22(4), 36–47, doi:10.5670/oceanog.2009.95, 2009.
- 518 Feng, Y., Hare, C. E., Leblanc, K., Rose, J. M., Zhang, Y., DiTullio, G. R., Lee, P. A., Wilhelm, S. W., Rowe, J. M., Sun, J.,
519 Nemcek, N., Gueguen, C., Passow, U., Benner, I., Brown, C., and Hutchins, D. A.: Effects of increased pCO₂ and temperature
520 on the North Atlantic spring bloom. I. The phytoplankton community and biogeochemical response, *Mar. Ecol. Prog. Ser.*,
521 388, 13–25, doi:10.3354/meps08133, 2009.
- 522 Ferland, J., Gosselin, M., and Starr, M.: Environmental control of summer primary production in the Hudson Bay system: The
523 role of stratification, *J. Mar. Syst.*, 88(3), 385–400, doi:10.1016/j.jmarsys.2011.03.015, 2011.
- 524 Gaaloul, H.: Effets du changement global sur les particules exopolymériques transparentes au sein de l’estuaire maritime du
525 Saint-Laurent, M.Sc. thesis, Université du Québec à Rimouski, Canada, 133 pp., 2017.
- 526 Galbraith, P. S., Chassé, J., Gilbert, D., Larouche, P., Caverhill, C., Lefaivre, D., Brickman, D., Pettigrew, B., Devine, L., and
527 Lafleur, C.: Physical Oceanographic Conditions in the Gulf of St. Lawrence in 2013, *DFO Can. Sci. Advis. Sec. Res. Doc.*,
528 2014/062(November), vi + 84 pp, 2014.
- 529 Gao, K., and Campbell, D. A.: Photophysiological responses of marine diatoms to elevated CO₂ and decreased pH: A review,
530 *Funct. Plant Biol.*, 41(5), 449–459, doi:10.1071/FP13247, 2014.
- 531 Gao, G., Jin, P., Liu, N., Li, F., Tong, S., Hutchins, D. A., and Gao, K.: The acclimation process of phytoplankton biomass,
532 carbon fixation and respiration to the combined effects of elevated temperature and pCO₂ in the northern South China Sea,
533 *Mar. Pollut. Bull.*, 118(1–2), 213–220, doi:10.1016/j.marpolbul.2017.02.063, 2017.
- 534 Gattuso, J. P., Mach, K. J., and Morgan, G.: Ocean acidification and its impacts: An expert survey, *Clim. Change*, 117(4),
535 725–738, doi:10.1007/s10584-012-0591-5, 2013.
- 536 Gattuso, J.-P., Magnan, A., Bille, R., Cheung, W. W. L., Howes, E. L., Joos, F., Allemand, D., Bopp, L., Cooley, S. R., Eakin,
537 C. M., Hoegh-Guldberg, O., Kelly, R. P., Portner, H.-O., Rogers, a. D., Baxter, J. M., Laffoley, D., Osborn, D., Rankovic, A.,
538 Rochette, J., Sumaila, U. R., Treyer, S., and Turley, C.: Contrasting futures for ocean and society from different anthropogenic
539 CO₂ emissions scenarios, *Science*, 349(6243), doi:10.1126/science.aac4722, 2015.



- 540 Giordano, M., Beardall, J., and Raven, J. A.: CO₂ concentrating mechanisms in algae: Mechanisms, environmental
541 modulation., and evolution, *Annu. Rev. Plant Biol.*, 56(1), 99–131, doi:10.1146/annurev.arplant.56.032604.144052, 2005.
- 542 Gunderson, A. R., Armstrong, E. J., and Stillman, J. H.: Multiple stressors in a changing World: The need for an improved
543 perspective on physiological responses to the dynamic marine environment, *Ann. Rev. Mar. Sci.*, 8(1), 357–378,
544 doi:10.1146/annurev-marine-122414-033953, 2016.
- 545 Hama, T., Inoue, T., Suzuki, R., Kashiwazaki, H., Wada, S., Sasano, D., Kosugi, N., and Ishii, M.: Response of a phytoplankton
546 community to nutrient addition under different CO₂ and pH conditions, *J. Oceanogr.*, 72(2), 207–223, doi:10.1007/s10872-
547 015-0322-4, 2016.
- 548 Hansen, H. P., and Koroleff, F.: Determination of nutrients, in: *Methods of Seawater Analysis*, 3, Eds: Grasshoff K., Kremling,
549 K., and Ehrhardt, M., Wiley-VCH Verlag GmbH, Weinheim, Germany, 159–228, doi:10.1002/9783527613984.ch10, 2007.
- 550 Hare, C. E., Leblanc, K., DiTullio, G. R., Kudela, R. M., Zhang, Y., Lee, P. A., Riseman, S., and Hutchins, D. A.: Consequences
551 of increased temperature and CO₂ for phytoplankton community structure in the Bering Sea, *Mar. Ecol. Prog. Ser.*, 352, 9–16,
552 doi:10.3354/meps07182, 2007.
- 553 Havenhand, J., Dupont, S., and Quinn, G. P.: Designing ocean acidification experiments to maximise inference, in *Guide to*
554 *best practices for ocean acidification research and data reporting*, Eds: Riebesell, U., Fabry, V. J., and Gattuso, J.-P.,
555 Publications Office of the European Union, Luxembourg, 67–80, 2010.
- 556 Hopkins, F. E., Turner, S. M., Nightingale, P. D., Steinke, M., Bakker, D., and Liss, P. S.: Ocean acidification and marine
557 trace gas emissions, *Proc. Natl. Acad. Sci. U.S.A.*, 107(2), 760–765, doi:10.1073/pnas.0907163107, 2010.
- 558 Hussherr, R., Levasseur, M., Lizotte, M., Tremblay, J. É., Mol, J., Thomas, H., Gosselin, M., Starr, M., Miller, L. A., Jarníková,
559 T., Schuback, N., and Mucci, A.: Impact of ocean acidification on Arctic phytoplankton blooms and dimethyl sulfide
560 concentration under simulated ice-free and under-ice conditions, *Biogeosciences*, 14(9), 2407–2427, doi:10.5194/bg-14-2407-
561 2017, 2017.
- 562 IPCC: Working Group I Contribution to the Fifth Assessment Report Climate Change 2013: The Physical Science Basis,
563 Intergov. Panel Clim. Chang., 1535, doi:10.1017/CBO9781107415324., 2013.
- 564 Kim, K. Y., Garbary, D. J., and McLachlan, J. L.: Phytoplankton dynamics in Pomquet Harbour, Nova Scotia: a lagoon in the
565 southern Gulf of St Lawrence, *Phycologica*, 43(3), 311–328, 2004.
- 566 Kim, J. H., Kim, K. Y., Kang, E. J., Lee, K., Kim, J. M., Park, K. T., Shin, K., Hyun, B., and Jeong, H. J.: Enhancement of
567 photosynthetic carbon assimilation efficiency by phytoplankton in the future coastal ocean, *Biogeosciences*, 10(11), 7525–
568 7535, doi:10.5194/bg-10-7525-2013, 2013.
- 569 Knap, A., Michaels, A., Close, A. R., Ducklow, H., and Dickson, A. G.: Protocols for the Joint Global Ocean Flux Study
570 (JGOFS) core measurements, JGOFS Rep No. 19, Reprint of the IOC Manuals and Guides No. 29, UNESCO, Bergen, Norway,
571 doi:10013/epic.27912, 1996.



- 572 Kroeker, K. J., Kordas, R. L., Crim, R., Hendriks, I. E., Ramajo, L., Singh, G. S., Duarte, C. M., and Gattuso, J. P.: Impacts of
573 ocean acidification on marine organisms: Quantifying sensitivities and interaction with warming, *Glob. Chang. Biol.*, 19(6),
574 1884–1896, doi:10.1111/gcb.12179, 2013.
- 575 Larouche, P., and Galbraith, P. S.: Canadian coastal seas and Great Lakes sea surface temperature climatology and recent
576 trends, *Can. J. Remote Sens.*, 42(3), 243–258, doi:10.1080/07038992.2016.1166041, 2016.
- 577 Law, C. S., Breitbarth, E., Hoffmann, L. J., McGraw, C. M., Langlois, R. J., Laroche, J., Marriner, A., and Safi, K. A.: No
578 stimulation of nitrogen fixation by non-filamentous diazotrophs under elevated CO₂ in the South Pacific, *Glob. Chang. Biol.*,
579 18, 3004–3014, 2012.
- 580 Le Quéré, C., Moriarty, R., Andrew, R. M., Canadell, J. G., Sitch, S., Korsbakken, J. I., Friedlingstein, P., Peters, G. P., andres,
581 R. J., Boden, T. A., Houghton, R. A., House, J. I., Keeling, R. F., Tans, P., Arneeth, A., Bakker, D. C. E., Barbero, L., Bopp,
582 L., Chang, J., Chevallier, F., Chini, L. P., Ciais, P., Fader, M., Feely, R. A., Gkritzalis, T., Harris, I., Hauck, J., Ilyina, T., Jain,
583 A. K., Kato, E., Kitidis, V., Klein Goldewijk, K., Koven, C., Landschützer, P., Lauvset, S. K., Lefèvre, N., Lenton, A., Lima,
584 I. D., Metzl, N., Millero, F., Munro, D. R., Murata, A., S. Nabel, J. E. M., Nakaoka, S., Nojiri, Y., O'Brien, K., Olsen, A.,
585 Ono, T., Pérez, F. F., Pfeil, B., Pierrot, D., Poulter, B., Rehder, G., Rödenbeck, C., Saito, S., Schuster, U., Schwinger, J.,
586 Séférian, R., Steinhoff, T., Stocker, B. D., Sutton, A. J., Takahashi, T., Tilbrook, B., Van Der Laan-Luijkx, I. T., Van Der
587 Werf, G. R., Van Heuven, S., Vandemark, D., Viovy, N., Wiltshire, A., Zaehle, S., and Zeng, N.: Global Carbon Budget 2015,
588 *Earth Syst. Sci. Data*, 7(2), 349–396, doi:10.5194/essd-7-349-2015, 2015.
- 589 Legendre, L., Demers, S., Yentsch, C. M., and Yentsch, C. S.: The ¹⁴C method: Patterns of dark CO₂ fixation and DCMU
590 correction to replace the dark bottle, *Limnol. Oceanogr.*, 28(5), 996–1003, doi:10.4319/lo.1983.28.5.0996, 1983.
- 591 Levasseur, M., Theriault, J.-C., and Legendre, L.: Hierarchical control of phytoplankton succession by physical factors, *Mar.*
592 *Ecol. Prog. Ser.*, 19, 211–222, doi:10.3354/meps019211, 1984.
- 593 Levasseur, M. E., and Theriault, J.-C.: Phytoplankton biomass and nutrient dynamics in a tidally induced upwelling: the role
594 of the NO₃:SiO₄ ratio, *Mar. Ecol. Prog. Ser.*, 39, 87–97, 1987.
- 595 Levasseur, M. E., Harrison, P. J., Heimdal, B. R., and Theriault, J.-C.: Simultaneous nitrogen and silicate deficiency of a
596 phytoplankton community in a coastal jet-front, *Mar. Biol.*, 104(2), 329–338, doi:10.1007/BF01313275, 1990.
- 597 Lomas, M. W., Hopkinson, B. M., Losh, J. L., Ryan, D. E., Shi, D. L., Xu, Y., and Morel, F. M. M.: Effect of ocean acidification
598 on cyanobacteria in the subtropical North Atlantic, *Aquat. Microb. Ecol.*, 66(3), 211–222, doi:10.3354/ame01576, 2012.
- 599 Lund, J. W. G., Kipling, C., and Le Cren, E. D.: The inverted microscope method of estimating algal numbers and the statistical
600 basis of estimates by counting, *Hydrobiologia*, 11, 143–170, 1958.
- 601 MacGilchrist, G. A., Shi, T., Tyrrell, T., Richier, S., Moore, C. M., Dumousseaud, C., and Achterberg, E. P.: Effect of enhanced
602 pCO₂ levels on the production of dissolved organic carbon and transparent exopolymer particles in short-term bioassay
603 experiments, *Biogeosciences*, 11(13), 3695–3706, doi:10.5194/bg-11-3695-2014, 2014.
- 604 Marie, D., Simon, N., and Vaultot, D.: Phytoplankton cell counting by flow cytometry, *Algal Cult. Tech.*, 253–267,
605 doi:10.1016/B978-012088426-1/50018-4, 2005.



- 606 Maugendre, L., Gattuso, J. P., Louis, J., De Kluijver, A., Marro, S., Soetaert, K., and Gazeau, F.: Effect of ocean warming and
607 acidification on a plankton community in the NW Mediterranean Sea, *ICES J. Mar. Sci.*, 72(6), 1744–1755,
608 doi:10.1093/icesjms/fsu161, 2015.
- 609 Millero, F. J.: The pH of estuarine waters, *Limnol. Oceanogr.*, 31(4), 839–847, doi:10.4319/lo.1986.31.4.0839, 1986.
- 610 Montagnes, D. J. S., and Franklin, M.: Effect of temperature on diatom volume, growth rate, and carbon and nitrogen content:
611 Reconsidering some paradigms, *Limnol. Oceanogr.*, 46(8), 2008–2018, doi:10.4319/lo.2001.46.8.2008, 2001.
- 612 Morán, X. A. G., Sebastián, M., Pedrós-Alió, C., and Estrada, M.: Response of Southern Ocean phytoplankton and
613 bacterioplankton production to short-term experimental warming, *Limnol. Oceanogr.*, 51(4), 1791–1800,
614 doi:10.4319/lo.2006.51.4.1791, 2006.
- 615 Morán, A. G., Alonso-sa, L., Nogueira, E., Ducklow, H. W., Gonza, N., Calvo-dí, A., Arandia-gorostidi, N., Di, L., Huete-
616 staufer, T. M., Rey, U., and Carlos, J.: More, smaller bacteria in response to ocean's warming?, *Proc. R. Soc.*, 282(1810), 1–
617 9, doi:http://dx.doi.org/10.1098/rspb.2015.0371, 2015.
- 618 Mucci, A., Levasseur, M., Gratton, Y., Martias, C., Scarratt, M., Gilbert, D., Tremblay, J.-É., Ferreyra, G., and Lansard, B.:
619 Tidally-induced variations of pH at the head of the Laurentian Channel, *Can. J. Fish. Aquat. Sci.*, doi:10.1139/cjfas-2017-
620 0007, 2017.
- 621 Neale, P. J., Sobrino, C., Segovia, M., Mercado, J. M., Leon, P., Cortés, M. D., Tuite, P., Picazo, A., Salles, S., Cabrerizo, M.
622 J., Prasil, O., Montecino, V., and Reul, A.: Effect of CO₂, nutrients and light on coastal plankton. I. Abiotic conditions and
623 biological responses, *Aquat. Biol.*, 22, 25–41, doi:10.3354/ab00587, 2014.
- 624 Parsons, T. R., Maita, Y., and Lalli, C. M.: A manual of chemical and biological methods for seawater analysis, Permagon
625 Press, New York, 1984.
- 626 Paul, C., Matthiessen, B., and Sommer, U.: Warming, but not enhanced CO₂ concentration, quantitatively and qualitatively
627 affects phytoplankton biomass, *Mar. Ecol. Prog. Ser.*, 528, 39–51, doi:10.3354/meps11264, 2015.
- 628 Paul, C., Sommer, U., Garzke, J., Moustaka-Gouni, M., Paul, A., and Matthiessen, B.: Effects of increased CO₂ concentration
629 on nutrient limited coastal summer plankton depend on temperature, *Limnol. Oceanogr.*, 61(3), 853–868,
630 doi:10.1002/lno.10256, 2016.
- 631 Pierrot, D., Lewis, E., and Wallace, D. W. R.: MS Excel program developed for CO₂ system calculations, Carbon Dioxide
632 Information Analysis Center, ORNL/CDIAC-105a, Oak Ridge National Laboratory, US Department of Energy, Oak Ridge,
633 592 Tennessee, 2006.
- 634 Raven, J. A., Beardall, J., and Giordano, M.: Energy costs of carbon dioxide concentrating mechanisms in aquatic organisms,
635 *Photosynth. Res.*, 121, 111–124, 2014.
- 636 Riebesell, U., and Gattuso, J.-P.: Lessons learned from ocean acidification research, *Nat. Clim. Chang.*, 5(1), 12–14,
637 doi:10.1038/nclimate2456, 2015.
- 638 Riebesell, U., and Tortell, P. D.: Effects of ocean acidification on pelagic organism and ecosystems, in *Ocean Acidification*,
639 Eds: Gattuso J.-P., and Hansson L., Oxford University Press, New York, 99–121, 2011.



- 640 Riebesell, U., Schulz, K. G., Bellerby, R. G. J., Botros, M., Fritsche, P., Meyerhöfer, M., Neill, C., Nondal, G., Oschlies, a,
641 Wohlers, J., and Zöllner, E.: Enhanced biological carbon consumption in a high CO₂ ocean., *Nature*, 450(7169), 545–548,
642 doi:10.1038/nature06267, 2007.
- 643 Riebesell, U., Czerny, J., Von Bröckel, K., Boxhammer, T., Büdenbender, J., Deckelnick, M., Fischer, M., Hoffmann, D.,
644 Krug, S. A., Lentz, U., Ludwig, A., Muche, R., and Schulz, K. G.: Technical Note: A mobile sea-going mesocosm system -
645 New opportunities for ocean change research, *Biogeosciences*, 10(3), 1835–1847, doi:10.5194/bg-10-1835-2013, 2013.
- 646 Robarts, R. D., and Zohary, T.: Temperature effects on photosynthetic capacity, respiration., and growth rates of bloom-
647 forming cyanobacteria, *New Zeal. J. Mar. Freshw. Res.*, 21(3), 391–399, doi:10.1080/00288330.1987.9516235, 1987.
- 648 Robert-Baldo, G., Morris, M., and Byrne, R.: Spectrophotometric determination of seawater pH using phenol red, *Anal. Chem.*,
649 3(57), 2564–2567, doi:10.1021/ac00290a030, 1985.
- 650 Rose, J. M., Feng, Y., Gobler, C. J., Gutierrez, R., Harel, C. E., Leblanc, K., and Hutchins, D. A.: Effects of increased pCO₂
651 and temperature on the North Atlantic spring bloom. II. Microzooplankton abundance and grazing, *Mar. Ecol. Prog. Ser.*, 388,
652 27–40, doi:10.3354/meps08134, 2009.
- 653 Roy, S., Chanut, J.-P., Gosselin, M., and Sime-Ngando, T.: Characterization of phytoplankton communities in the Lower St.
654 Lawrence Estuary using HPLC-detected pigments and cell microscopy, *Mar. Ecol. Prog. Ser.*, 142, 55–73,
655 doi:10.3354/meps142055, 1996.
- 656 Sala, M. M., Aparicio, F. L., Balagué, V., Boras, J. A., Borrull, E., Cardelús, C., Cros, L., Gomes, A., López-Sanz, A., Malits,
657 A., Martinez, R. A., Mestre, M., Movilla, J., Sarmiento, H., Vázquez-Domínguez, E., Vaqué, D., Pinhassi, J., Calbet, A., Calvo,
658 E., Gasol, J. M., Pelejero, C., and Marrasé, C.: Contrasting effects of ocean acidification on the microbial food web under
659 different trophic conditions, *ICES J. Mar. Sci.*, 73(3), 670–679, doi:10.1093/icesjms/fsv130, 2016.
- 660 Schulz, K. G., Bellerby, R. G. J., Brussaard, C. P. D., Büdenbender, J., Czerny, J., Engel, A., Fischer, M., Koch-Klavsen, S.,
661 Krug, S. A., Lischka, S., Ludwig, A., Meyerhöfer, M., Nondal, G., Silyakova, A., Stühr, A., and Riebesell, U.: Temporal
662 biomass dynamics of an Arctic plankton bloom in response to increasing levels of atmospheric carbon dioxide, *Biogeosciences*,
663 10(1), 161–180, doi:10.5194/bg-10-161-2013, 2013.
- 664 Schulz, K. G., Bach, L. T., Bellerby, R. G. J., Bermudez, R., Budenbender, J., Boxhammer, T., Czerny, J., Engel, A., Ludwig,
665 A., Meyerhofer, M., Larsen, A., Paul, A., Sswat, M., and Riebesell, U.: Phytoplankton blooms at increasing levels of
666 atmospheric carbon dioxide: experimental evidence for negative effects on prymnesiophytes and positive on small
667 picoeukaryotes, *Front. Mar. Sci.*, 4, 64, doi:10.3389/fmars.2017.00064, 2017.
- 668 Sommer, U., and Lengfellner, K.: Climate change and the timing, magnitude, and composition of the phytoplankton spring
669 bloom, *Glob. Chang. Biol.*, 14(6), 1199–1208, doi:10.1111/j.1365-2486.2008.01571.x, 2008.
- 670 Sommer, U., Paul, C., and Moustaka-Gouni, M.: Warming and ocean acidification effects on phytoplankton - From species
671 shifts to size shifts within species in a mesocosm experiment, *PLoS ONE*, 10(5), 17, doi:10.1371/journal.pone.0125239, 2015.
- 672 Starr, M., St-Amand, L., Devine, L., Bérard-Therriault, L., and Galbraith, P. S.: State of phytoplankton in the Estuary and Gulf
673 of St. Lawrence during 2003, *CSAS Res. Doc.*, 2004/123, 35, 2004.



- 674 Suzuki, Y., and Takahashi, M.: Growth responses of several diatom species isolated from various environments to temperature,
675 J. Phycol., 31(6), 880–888, doi:10.1111/j.0022-3646.1995.00880.x, 1995.
- 676 Tatters, A. O., Roleda, M. Y., Schnetzer, A., Fu, F., Hurd, C. L., Boyd, P. W., Caron, D. A., Lie, A. A. Y., Hoffmann, L. J.,
677 and Hutchins, D. A.: Short- and long-term conditioning of a temperate marine diatom community to acidification and
678 warming., Philos. Trans. R. Soc. Lond. B. Biol. Sci., 368(1627), 20120437, doi:10.1098/rstb.2012.0437, 2013.
- 679 Taylor, A. H., Harbour, D. S., Harris, R. P., Burkill, P. H., and Edwards, E. S.: Seasonal succession in the pelagic ecosystem
680 of the North Atlantic and the utilization of nitrogen, J. Plankton Res., 15(8), 875–891, doi:10.1093/plankt/15.8.875, 1993.
- 681 Thomas, M. K., Kremer, C. T., Klausmeier, C. a and Litchman, E.: A global pattern of thermal adaptation in marine
682 phytoplankton., Science, 338(6110), 1085–1088, doi:10.1126/science.1224836, 2012.
- 683 Todgham, A. E., and Stillman, J. H.: Physiological responses to shifts in multiple environmental stressors: Relevance in a
684 changing world, Integr. Comp. Biol., 53(4), 539–544, doi:10.1093/icb/ict086, 2013.
- 685 Tomas, C. R. (ed): Identifying Marine Phytoplankton, Academic Press: San Diego, 858 pp., 1997.
- 686 Tortell, P. D., DiTullio, G. R., Sigman, D. M., and Morel, F. M. M.: CO₂ effects on taxonomic composition and nutrient
687 utilization in an Equatorial Pacific phytoplankton assemblage, Mar. Ecol. Prog. Ser., 236, 37–43, doi:10.3354/meps236037,
688 2002.
- 689 Trimborn, S., Wolf-Gladrow, D., Richter, K. U., and Rost, B.: The effect of pCO₂ on carbon acquisition and intracellular
690 assimilation in four marine diatoms, J. Exp. Mar. Bio. Ecol., 376(1), 26–36, doi:10.1016/j.jembe.2009.05.017, 2009.
- 691 Wijffels, S., Roemmich, D., Monselesan, D., Church, J., and Gilson, J.: Ocean temperatures chronicle the ongoing warming
692 of Earth, Nat. Clim. Chang., 6(2), 116–118, doi:10.1038/nclimate2924, 2016.
- 693 Wu, Y., Gao, K., and Riebesell, U.: CO₂-induced seawater acidification affects physiological performance of the marine diatom
694 *Phaeodactylum tricornutum*, Biogeosciences, 7(9), 2915–2923, doi:10.5194/bg-7-2915-2010, 2010.
- 695 Yoshimura, T., Nishioka, J., Suzuki, K., Hattori, H., Kiyosawa, H., and Watanabe, Y. W.: Impacts of elevated CO₂ on organic
696 carbon dynamics in nutrient depleted Okhotsk Sea surface waters, J. Exp. Mar. Bio. Ecol., 395(1–2), 191–198,
697 doi:10.1016/j.jembe.2010.09.001, 2010.
- 698 Yoshimura, T., Sugie, K., Endo, H., Suzuki, K., Nishioka, J., and Ono, T.: Organic matter production response to CO₂ increase
699 in open subarctic plankton communities: Comparison of six microcosm experiments under iron-limited and -enriched bloom
700 conditions, Deep Res. Part I Oceanogr. Res. Pap., 94, 1–14, doi:10.1016/j.dsr.2014.08.004, 2014.

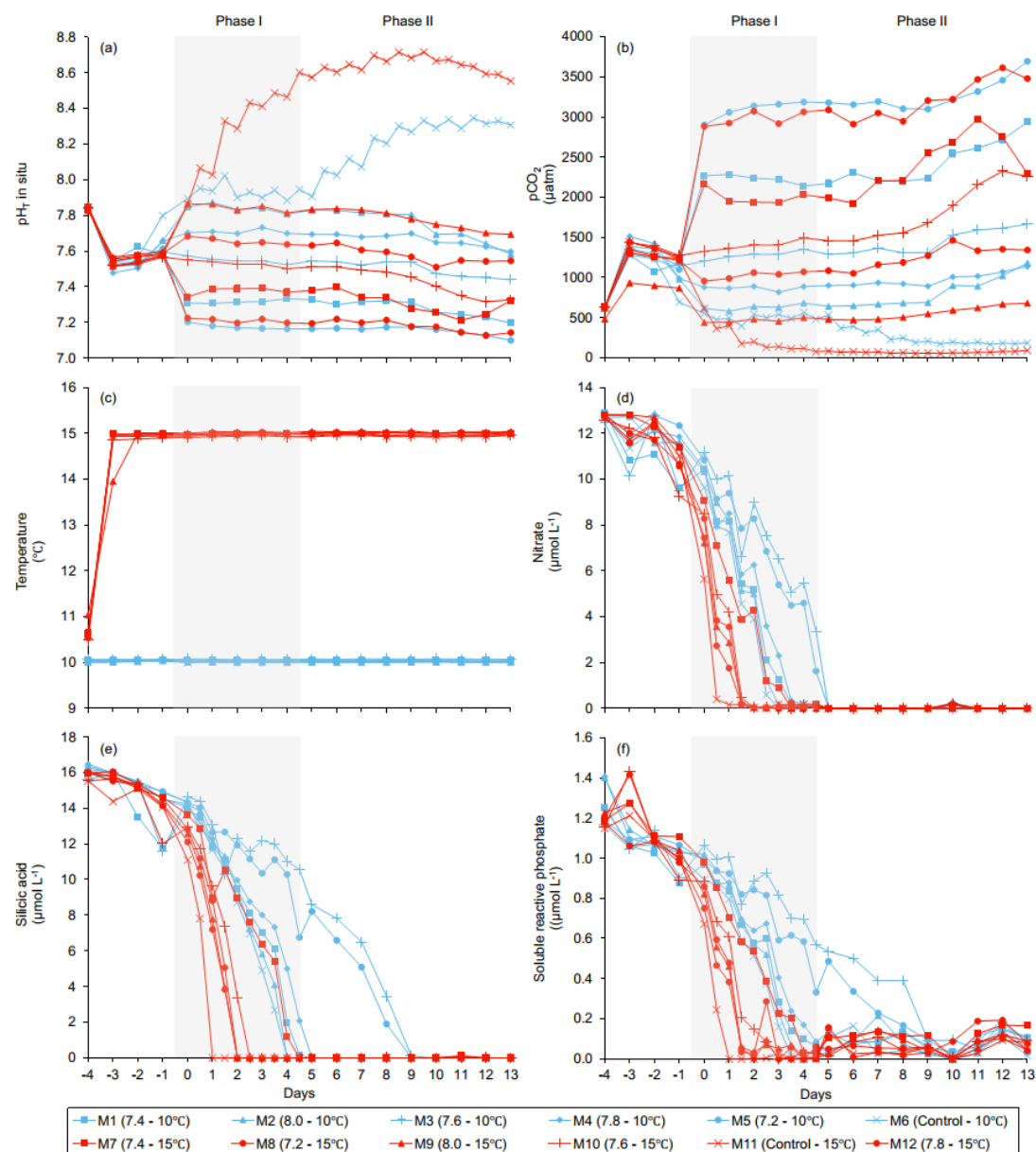


Figure 1. Temporal variations over the course of the experiment for: (a) pH_T , (b) pCO_2 , (c) temperature, (d) nitrate, (e) silicic acid, (f) soluble reactive phosphate. For symbol attribution to treatments, see legend.

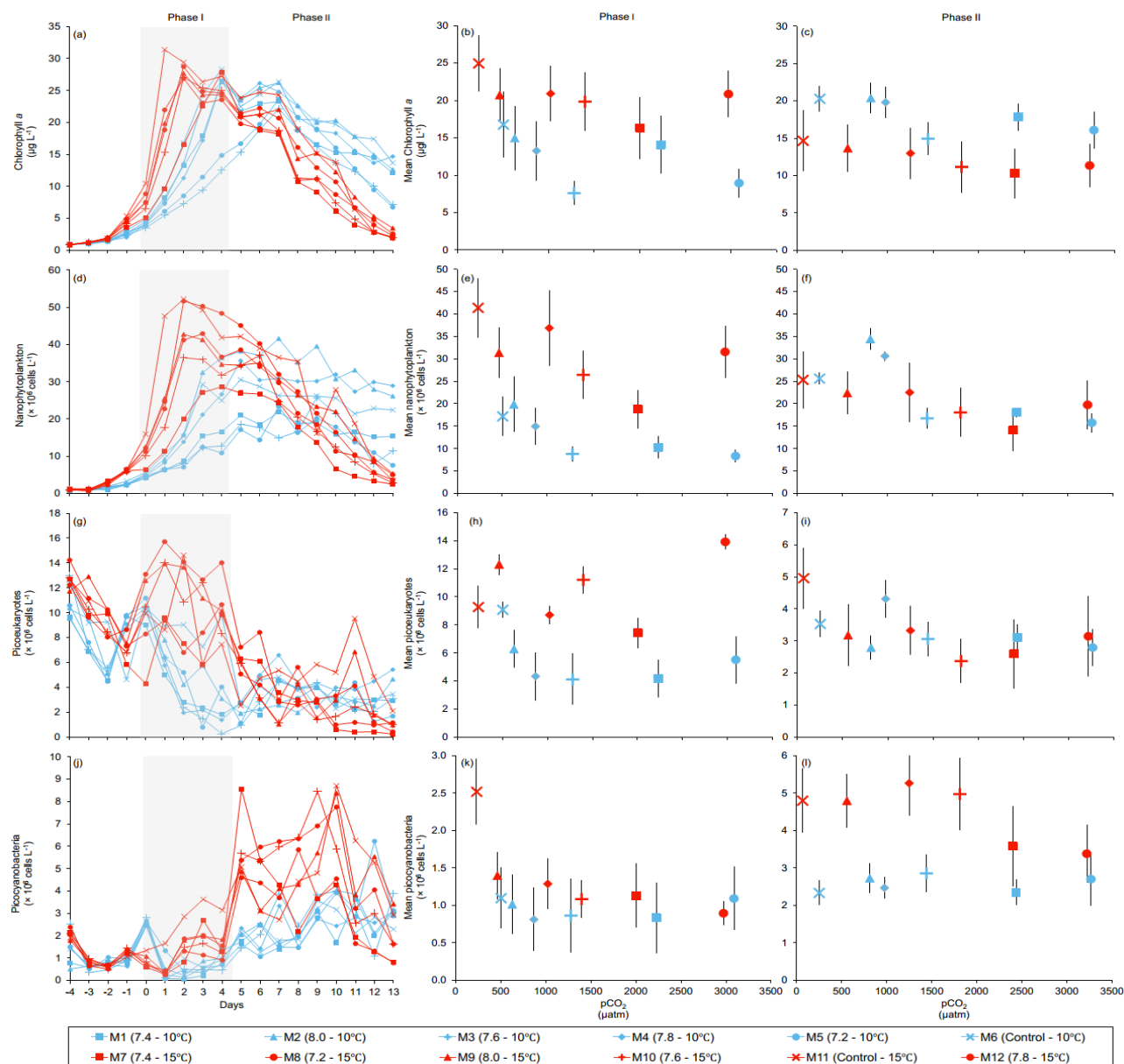


Figure 2. Temporal variations, and averages \pm SE during Phase I (day 0 to day 4) and Phase II (day 5 to day 13) for: (a-c) chlorophyll *a*, (d-f) nanophytoplankton, (g-i) picoeukaryotes, (j-l) picocyanobacteria. For symbol attribution to treatments, see legend.

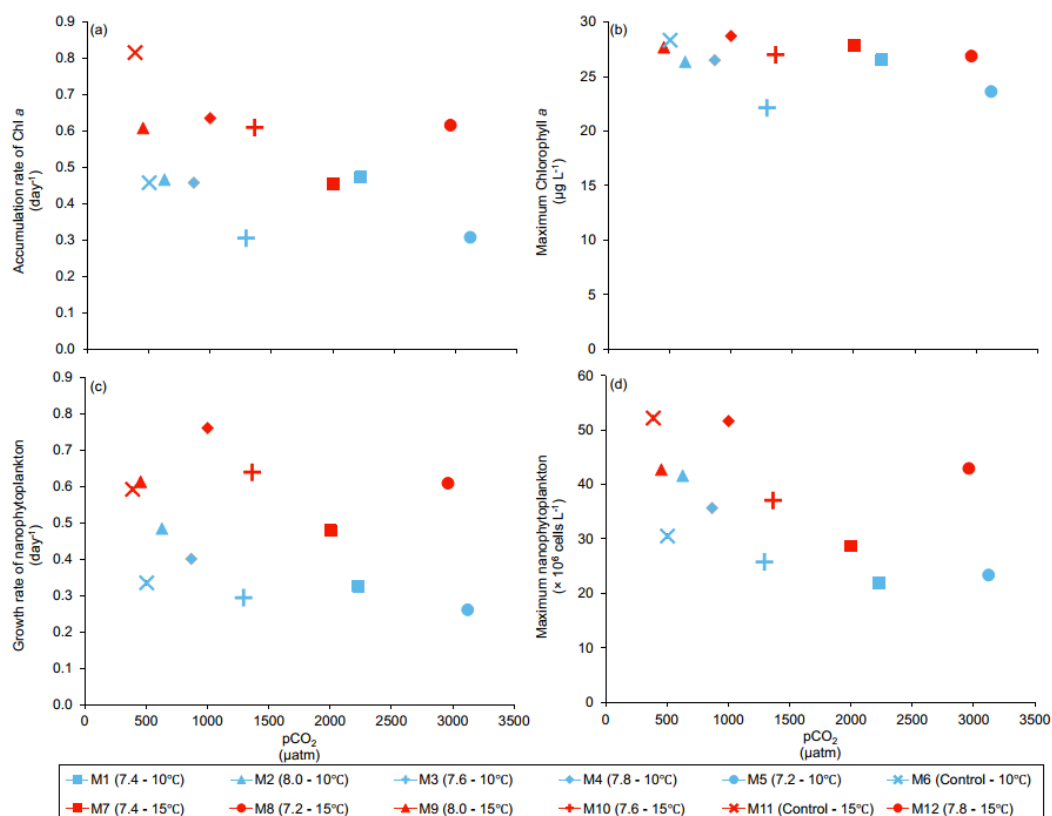


Figure 3. (a) Accumulation rate of Chl *a* (day 0 to maximum Chl *a* concentration), (b) maximum Chl *a* concentrations, (c) growth rate of nanophytoplankton (day 0 to maximum nanophytoplankton abundance), and (d) maximum nanophytoplankton abundance during the experiment. For symbol attribution to treatments, see legends.

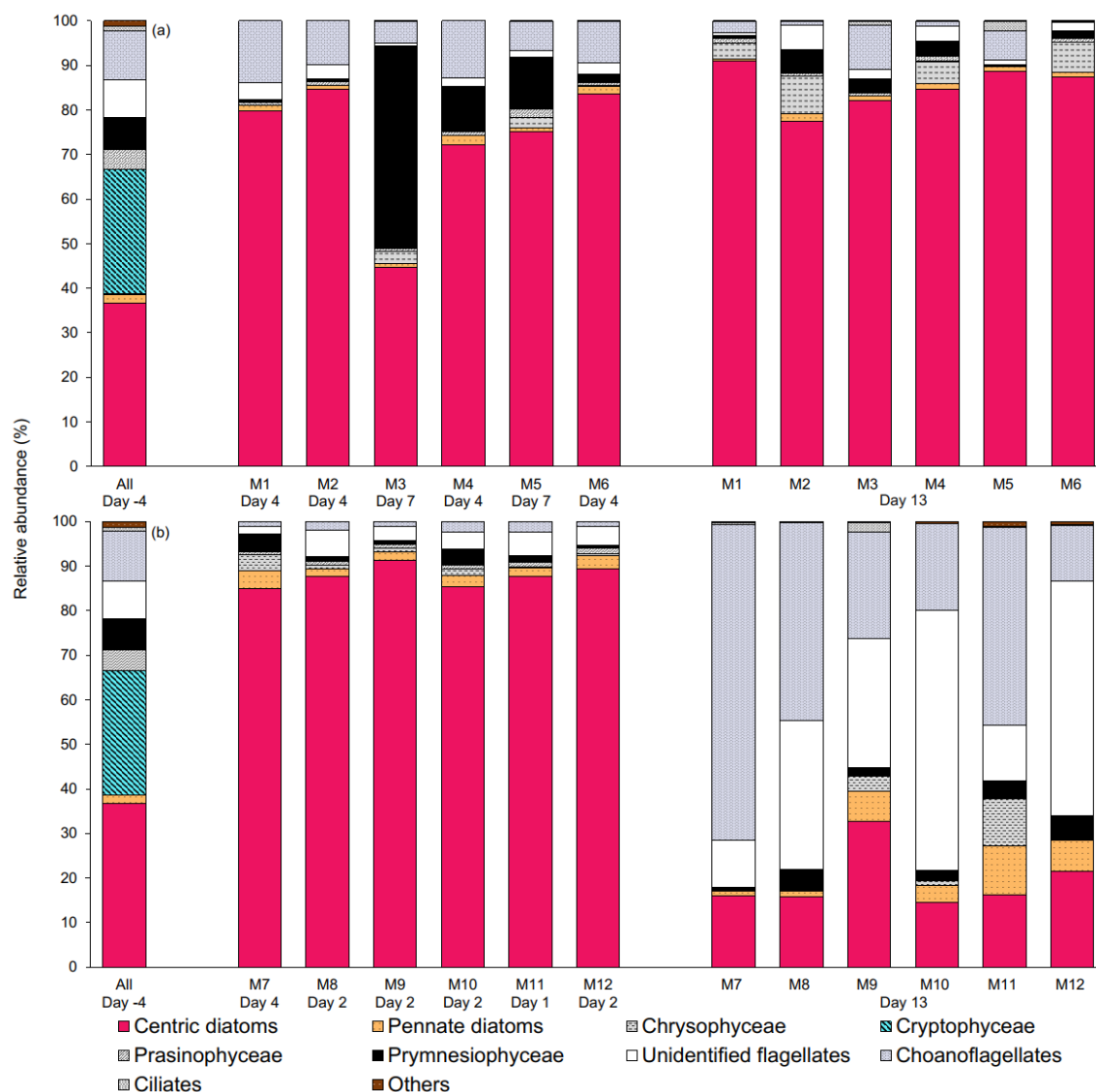


Figure 4. Relative abundance of 10 groups of protists at the beginning of the experiment (day -4), on the day of maximum Chl *a* concentrations in each mesocosm, and at the end of the experiment (day 13) for (a) 10 °C and (b) 15 °C mesocosms. The group « others » include dinoflagellates, Chlorophyceae, Dictyochophyceae, Euglenophyceae, heterotrophic groups, and unidentified cells. Each bar plot represents a mesocosm at a given time. The bar plot on day -4 represents the initial community assemblage before temperature manipulation and acidification, and is therefore the same for each temperature treatment. For symbol attribution to treatments, see legend.

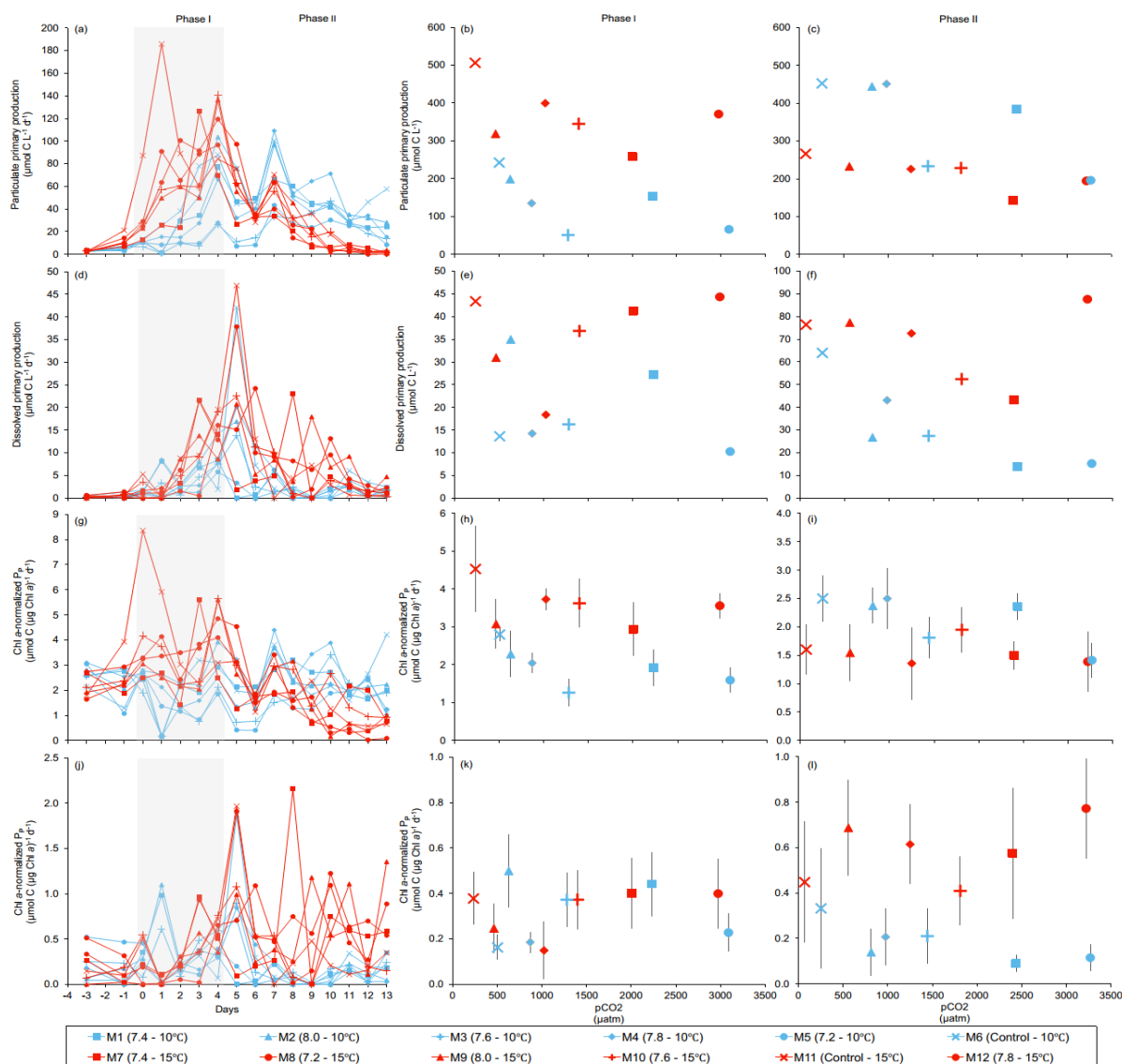


Figure 5. Temporal variations, time-integrated or averaged \pm SE during Phase I (day 0 to day 4) and Phase II (day 5 to day 13) for: (a-c) particulate primary production, (d-f) dissolved primary production, (g-i) Chl *a*-normalized particulate primary production, (j-l) Chl *a*-normalized dissolved primary production. For symbol attribution to treatments, see legend.

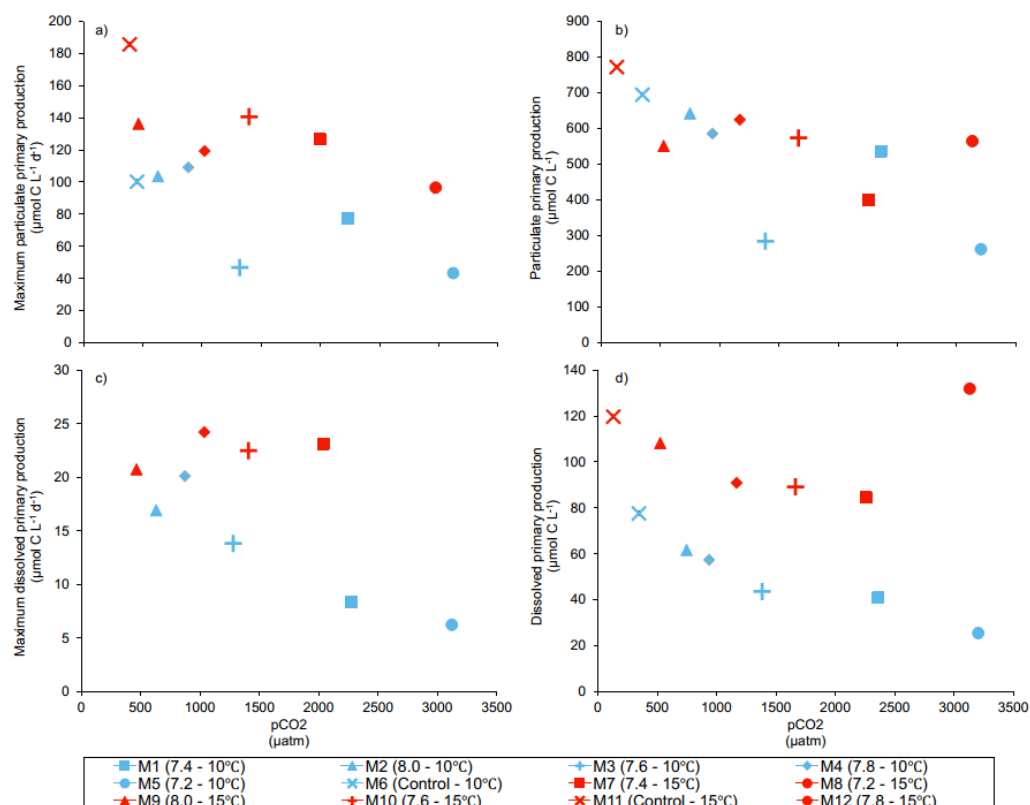


Figure 6. (a) Maximum particulate primary production, (b) time-integrated particulate primary production (c) maximum dissolved primary production, and (d) time-integrated dissolved primary production over the full course of the experiment (day 0 to day 13). For symbol attribution to treatments, see legend.



Table 1. Results of the generalized least squares models (gls) tests for the effects of temperature, pCO₂, and their interaction during Phase I (day 0 to day 4). Separate analysis with pCO₂ as a continuous factor were performed when temperature had a significant effect. Chl *a* concentration, nanophytoplankton abundance, picoeukaryote abundance, picocyanobacteria abundance, particulate and dissolved primary production, and Chl *a*-normalized particulate and dissolved primary production. Significant results are in bold. **p* < 0.05.

Response Variable	Factor	df	t-value	p-value
Mean Chl <i>a</i> concentration (µg L ⁻¹)	Temperature	8	2.307	0.050*
	pCO ₂ (10 °C)	4	-1.362	0.245
	pCO ₂ (15 °C)	4	-1.263	0.275
Mean nanophytoplankton abundance (× 10 ⁶ cells L ⁻¹)	Temperature	8	2.980	0.018*
	pCO ₂ (10 °C)	4	-2.729	0.053
	pCO ₂ (15 °C)	4	-1.231	0.286
Mean picoeukaryote abundance (× 10 ⁶ cells L ⁻¹)	Temperature	8	1.157	0.281
	pCO ₂	8	-1.070	0.316
	pCO ₂ × Temperature	8	1.085	0.309
Mean picocyanobacteria abundance (× 10 ⁶ cells L ⁻¹)	Temperature	8	3.066	0.015*
	pCO ₂ (10 °C)	4	0.125	0.907
	pCO ₂ (15 °C)	4	-2.268	0.086
Particulate primary production (µmol C L ⁻¹)	Temperature	8	2.690	0.028*
	pCO ₂ (10 °C)	4	-1.617	0.181
	pCO ₂ (15 °C)	4	-0.992	0.378
Dissolved primary production (µmol C L ⁻¹)	Temperature	8	0.756	0.472
	pCO ₂	8	-0.901	0.394
	pCO ₂ × Temperature	8	0.956	0.367
Chl <i>a</i> -normalized particulate primary production (µmol C (µg Chl <i>a</i>) ⁻¹ d ⁻¹)	Temperature	8	2.592	0.032*
	pCO ₂ (10 °C)	4	-1.467	0.216
	pCO ₂ (15 °C)	4	-0.840	0.448



Chl <i>a</i> -normalized dissolved primary production ($\mu\text{mol C } (\mu\text{g Chl } a)^{-1} \text{ d}^{-1}$)	Temperature	8	-0.350	0.735
	pCO ₂	8	-0.397	0.702
	pCO ₂ × Temperature	8	0.522	0.616



Table 2. Results of the generalized least squares models (glms) tests for the effects of temperature, pCO₂ and their interaction. Separate analysis with pCO₂ as a continuous factor were performed when temperature had a significant effect. Accumulation rate of Chl *a* (day 0 to maximum Chl *a* concentration), maximum Chl *a* concentration, growth rate of nanophytoplankton (day 0 to maximum nanophytoplankton abundance), and maximum nanophytoplankton abundance. Significant results are in bold. *p < 0.05.

Response Variable	Factor	df	t-value	p-value
Accumulation rate of Chl <i>a</i> (day ⁻¹)	Temperature	8	2.679	0.028*
	pCO ₂ (10 °C)	4	-1.476	0.214
	pCO ₂ (15 °C)	4	-1.759	0.154
Maximum Chl <i>a</i> concentration (µg L ⁻¹)	Temperature	8	1.305	0.228
	pCO ₂	8	-0.387	0.709
	pCO ₂ × Temperature	8	0.022	0.983
Growth rate of nanophytoplankton (day ⁻¹)	Temperature	8	2.534	0.035*
	pCO ₂ (10 °C)	4	-0.882	0.403
	pCO ₂ (15 °C)	4	0.601	0.564
Maximum nanophytoplankton abundance (× 10 ⁶ cells L ⁻¹)	Temperature	8	1.380	0.205
	pCO ₂	8	-0.735	0.484
	pCO ₂ × Temperature	8	0.302	0.770



Table 3. Results of the generalized least squares models (gls) tests for the effects of temperature, pCO₂, and their interaction during Phase II (day 5 to day 13). Separate analysis with pCO₂ as a continuous factor were performed when temperature had a significant effect. Chl *a* concentration, nanophytoplankton abundance, picoeukaryote abundance, picocyanobacteria abundance, particulate and dissolved primary production, and Chl *a*-normalized particulate and dissolved primary production. Significant results are in bold. **p* < 0.05, *p* < 0.01, ****p* < 0.001.**

Response Variable	Factor	df	t-value	p-value
Mean Chl <i>a</i> concentration (μg L ⁻¹)	Temperature	8	-3.600	0.007**
	pCO ₂ (10 °C)	4	-2.724	0.073
	pCO ₂ (15 °C)	4	-1.263	0.275
Mean nanophytoplankton abundance (× 10 ⁶ cells L ⁻¹)	Temperature	8	-1.465	0.181
	pCO ₂	8	-1.539	0.162
	pCO ₂ × Temperature	8	1.003	0.345
Mean picoeukaryotes abundance (× 10 ⁶ cells L ⁻¹)	Temperature	8	0.581	0.577
	pCO ₂	8	0.294	0.776
	pCO ₂ × Temperature	8	-0.698	0.505
Mean picocyanobacteria abundance (× 10 ⁶ cells L ⁻¹)	Temperature	8	6.107	<0.001***
	pCO ₂ (10 °C)	4	0.401	0.709
	pCO ₂ (15 °C)	4	-2.347	0.079
Particulate primary production (μmol C L ⁻¹)	Temperature	8	-2.248	0.012*
	pCO ₂ (10 °C)	4	-2.186	0.094
	pCO ₂ (15 °C)	4	-2.390	0.075
Dissolved primary production (μmol C L ⁻¹)	Temperature	8	1.154	0.282
	pCO ₂	8	-1.701	0.127
	pCO ₂ × Temperature	8	1.369	0.208
Chl <i>a</i> -normalized particulate primary production (μmol C (μg Chl <i>a</i>) ⁻¹ d ⁻¹)	Temperature	8	-3.387	0.010**
	pCO ₂ (10 °C)	4	-2.226	0.090
	pCO ₂ (15 °C)	4	-0.366	0.733



Chl <i>a</i> -normalized dissolved primary production ($\mu\text{mol C } (\mu\text{g Chl } a)^{-1} \text{ d}^{-1}$)	Temperature	8	1.973	0.073
	pCO ₂	8	-1.838	0.103
	pCO ₂ × Temperature	8	1.860	0.100



Table 4. Results of the generalized least squares models (glms) tests for the effects of temperature, pCO₂ and their interaction. Separate analysis with pCO₂ as a continuous factor were performed when temperature had a significant effect. Maximum particulate and dissolved primary production, and time-integration over the full duration of the experiment (day 0 to day 13). Natural logarithm transformation is indicated in parentheses when necessary, significant results are in bold. *p < 0.05, **p < 0.01.

Response Variable	Factor	Df	t-value	p-value
Maximum particulate primary production ($\mu\text{mol C L}^{-1} \text{ d}^{-1}$)	Temperature	8	2.466	0.039*
	pCO ₂ (10 °C)	4	-2.328	0.080
	pCO ₂ (15 °C)	4	-2.394	0.075
Time-integrated particulate primary production ($\mu\text{mol C L}^{-1} \text{ d}^{-1}$)	Temperature	8	-0.055	0.958
	pCO ₂ (10 °C)	4	-1.300	0.230
	pCO ₂ (15 °C)	4	0.801	0.446
(Log) Maximum dissolved primary production ($\mu\text{mol C L}^{-1}$)	Temperature	8	-0.659	0.528
	pCO ₂	8	-3.342	0.010**
	pCO ₂ × Temperature	8	2.858	0.021*
Time-integrated dissolved primary production ($\mu\text{mol C L}^{-1}$)	Temperature	8	1.687	0.130
	pCO ₂	8	-2.153	0.063
	pCO ₂ × Temperature	8	1.880	0.097